Scientific Reports

https://doi.org/10.1038/s41598-026-60211-8

Article in Press

Pioneer vegetation shapes soil microbial community assembly and ecosystem functions in riparian sand mining sites

Received: 8 April 2026

Accepted: 25 June 2026

Published online: 19 July 2026

Cite this article as: Yan T., Wang Z., Shan Y. *et al.* Pioneer vegetation shapes soil microbial community assembly and ecosystem functions in riparian sand mining sites. *Sci Rep* (2026). https://doi.org/10.1038/s41598-026-60211-8

Tengfei Yan, Zhengxin Wang, Yanxiang Shan, Jing Wang, Daochun Liu, Yevheniia Kremenetska & Xiang Lv

Pioneer Vegetation Shapes Soil Microbial Community Assembly and Ecosystem Functions in Riparian Sand Mining Sites

Tengfei Yan[1,4], Zhengxin Wang[1,2], Yanxiang Shan[3], Jing Wang[1], Daochun Liu[1], Yevheniia Kremenetska [5], Xiang Lv[1]*

1 Xinyang Huai River Catchment Riparian Zone Carbon Neutralization Engineering Technology, Xinyang Agriculture and Forestry University, Xinyang 464000, China

2 School of Resource and Environment, Henan Institute of Science and Technology, Xinxiang 453000, China

3 Henan Jigongshan Forest Ecosystem Observation and Research Station, The Forest Science Research Institute of Xinyang, Xinyang 464031, China;

4 Xinyang Ecological Research Institute, Xinyang 464000, China

5 Sumy national agrarian university, Sumy 40000, Ukraine

Tengfei Yan: (E-mail: 2011290003@xyafu.edu.cn)

Address: Xinyang Agriculture and Forestry University, No.1, Beihuan Road, Pingqiao District, Xinyang City, 464000, Henan, China

Zhengxin Wang: (E-mail: 15838983168@163.com)

Address: Xinyang Agriculture and Forestry University, No.1, Beihuan Road, Pingqiao District, Xinyang City, 464000, Henan, China

Yanxiang Shan: (E-mail: hnxysyx@163.com)

Address: Xinyang Academy of Agricultural Sciences, No. 20 Minquan South Street, Shihe District, Xinyang City, 464301, Henan, China

Jing Wang: (E-mail: jingjingw328@163.com)

Address: Xinyang Agriculture and Forestry University, No.1, Beihuan Road, Pingqiao District, Xinyang City, 464000, Henan, China

Daochun Liu: (E-mail: liudc2024@163.com)

Address: Xinyang Agriculture and Forestry University, No.1, Beihuan Road, Pingqiao District, Xinyang City, 464000, Henan, China

Yevheniia Kremenetska: (E-mail: e.kremenetska@gmail.com)

Address: Sumy National Agrarian University, No. 160, Herasyma, Kondratieva Street, Sumy, 40000, Ukraine

Xiang Lv: (*Corresponding author, E-mail: lvxiang1228@126.com)

Address: Xinyang Agriculture and Forestry University, No.1, Beihuan Road, Pingqiao District, Xinyang City, 464000, Henan, China

Abstract: Pioneer vegetation initiates the recovery of degraded ecosystem; However, its influence on soil microbial communities in riparian sand mining sites remains poorly understood. Four naturally established pioneer plant species

(*Artemisia scoparia*, *Imperata cylindrica*, *Saccharum arundinaceum*, and solitary trees) were selected in a representative sand mining site along the Huai River, and systematically investigated soil microbial community structure, assembly processes, co-occurrence network stability, and functional potential to elucidate the regulatory mechanisms of pioneer vegetation on soil microbial communities and ecosystem functions. The results showed that pioneer vegetation types shaped distinct soil microbial communities, with bacterial communities more responsive than fungi. Total carbon (TC), total phosphorus (TP), and nitrate nitrogen (NO_3-N) collectively explaining 76.8% of the variation in bacterial community composition. Microbial community composition exhibited strong vegetation-specific patterns. *A. scoparia* plots significantly enriched *Actinobacteria*, whereas solitary tree plots significantly enriched *Basidiomycota*. Network stability varied markedly with vegetation type; Functional prediction revealed that bacterial nitrogen cycling potential was significantly modulated by vegetation type, with nitrification potential being significantly lowest in *I. cylindrica*. Structural equation modeling demonstrated that vegetation type indirectly influenced soil multifunctionality via regulating soil physical properties, with contrasting pathways in bacterial and fungal models. Our findings suggest potential ecological mechanisms by which pioneer plants influence early ecosystem recovery in degraded riparian zones through the “plant-soil-microbe” continuum, thus providing a scientific basis for functional trait-based ecological restoration.

Keywords: Ecological restoration; Community assembly; Network stability; Function prediction; Soil multifunctionality

Introduction

Riparian corridors serve as critical ecotones linking aquatic and terrestrial ecosystems, delivering irreplaceable ecological functions, providing habitats, sustaining biodiversity, purifying pollutants, and stabilizing riverbank (Graziano et al. 2022; Singh et al. 2021). However, these vulnerable interfaces are increasingly degraded by intensive anthropogenic activities, among which large-scale instream sand mining has emerged as one of the most destructive. Unregulated extraction of sand mining has become a globe environmental crisis, imposing unprecedented pressure on river systems worldwide (Torres et al. 2017; Fritts. 2019). Intensive sand mining directly excavates riverbeds and banks, disrupting hydrological connectivity, altering geomorphological, and complete destroying original vegetation and soil layers. The resulting “sand mining sites” are characterized by severely disturbed physical structure and extreme depletion of organic matter and nutrients (Koehnken et al. 2020; Pandey et al. 2023). Restoring these highly degraded habitats requires a mechanistic understanding of the key pathways and drivers governing soil fertility reconstruction and ecosystem functions recovery during early restoration.

Pioneer plants function as ecosystem engineers that initiate early succession (Miller and Lane. 2019). They improve microclimate and soil structure, while directly and indirectly regulating soil physicochemical properties and biological activity through root exudates and litter inputs (Li et al. 2021). Importantly, different pioneer species exert differential effects on the soil environment due to their distinct life forms, root architecture, and litter chemistry, steering ecosystem recovery along divergent trajectories (Sun et al. 2018; Cacace et al. 2022). Azeria et al. (2020) showed directional convergence of understory traits in reclaimed forest wellsite over a 7-48 years chronosequence; Pioneer plants facilitate habitat recovery through multiple mechanisms. Their fibrous and adventitious roots enhance soil pore

structure and stability (Wu et al. 2021; Cacace et al. 2022), while root exudates and decomposing litter input organic carbon and nutrients, thereby altering soil carbon and nitrogen cycling and their associated microbial communities (Esperschütz et al. 2013; Yan et al. 2018). Indeed, the dynamics of dissolved organic carbon, total carbon, and nitrogen pools are often closely tied to pioneer colonization (Martínez-Garza et al. 2016; Cabrera Rodríguez et al. 2022). Moreover, pioneer plants typically exhibit strong growth, extensive root distribution, and high stress tolerance that enable successful establishment in nutrient-poor, degraded substrates (Ciccazzo et al. 2014; Li et al. 2021). Surveys indicate that pioneer species possess higher stem glucose content and chloroplast pigment concentrations, larger vessel elements and stomatal density than non-pioneers (Macieira et al. 2020). Thus, the species composition and trait spectra of pioneer plants largely determine the direction and pace of early succession, create favorable conditions for subsequent species colonization.

Soil microbial communities serve as sensitive indicators of ecosystem recovery, as their reassembly directly underpins nutrient cycling, organic matter decomposition, and soil aggregation (Venson et al. 2017; Bhaduri et al. 2022; Peddle et al. 2025). According to the hierarchical filtering framework, microbial community assembly in degraded habitats such as sand mining sites is regulated by hierarchical ecological filters (Hu et al. 2019; Wang et al. 2023). The initial filter is harsh abiotic conditions (low organic matter, coarse texture, nutrient depletion) select for only the most tolerant taxa. Subsequently, pioneer vegetation imposes a biotic filter, shaping distinct microhabitats through species-specific root exudates, litter quality, and rhizodeposition, selectively enriching or suppressing microbial groups and directing assembly trajectories (Rousk and Frey. 2015; Zhalnina et al. 2018). For example, in high-mountain environments, Ciccazzo et al., (2014) found that different pioneer plant species recruited distinct rhizosphere bacterial communities. Similarly, Zhang et al., (2021) propose that plant species outweighed biomass in determined soil microbial properties. In contrast, Ye et al. (2021) found that plant species identity per se weakly differentiated microbial communities, whereas plant functional traits (particularly aboveground biomass and coverage) were more important correlates, suggesting convergent microbial effects through similar traits. Hence, pioneer vegetation type emerges as a key determinant of microbial succession pathways, exerting long-lasting effects on recovery trajectories. However, current understanding of plant-microbe interactions derives primarily from forests, grasslands, or conventional mines, with limited attention to riparian sand mining sites (Markowicz et al. 2015; Azeria et al. 2020; Zhu et al. 2022). These habitats feature homogeneous substrates, frequent hydrological disturbance, and absent soil structure, potentially weakening or altering plant regulation of microbial communities (Akanwa. 2020; Rentier and Cammeraat. 2022). Nevertheless, it remains unclear whether abiotic filters homogenize microbial communities in riparian sand mining sites, or whether different pioneer plants can still engineer distinct microbial assemblages.

To address this knowledge gap, we conducted a field study in a representative sand mining site along the Huai River, focusing on four naturally established pioneer vegetation types (*Artemisia scoparia*, *Saccharum arundinaceum*, *Imperata cylindrica*, Solitary trees*)*. These species represent distinct life forms and are hypothesized to represent different successional stages (space-for-time assumption) (Miao et al., 2018; Lovell et al., 2023), providing an ideal natural experimental system to investigate plant-specific effects on soil microbial community structure and

functions. Specifically, we aimed to (i) characterize soil microbial diversity, composition, co-occurrence network attributes and keystone taxa under different pioneer vegetation types in sand mining sites; (ii) identify the key environmental drivers shaping the microbial composition of different pioneer vegetation in sand mining sites; (iii) elucidate the pathways through which pioneer plants influence soil multifunctionality via the plant-soil-microbial continuum. Building on the hierarchical filtering framework, we test two core hypotheses (H1) despite strong abiotic homogenization, different pioneer vegetation types impose distinct biotic filters that drive differentiation in microbial communities and interaction network; and (H2) these vegetation effects are mediated by soil physicochemical properties, which in turn influence soil multifunctionality. This study provides empirical evidence for understanding early restoration processes in riparian ecosystems subjected to intense anthropogenic disturbance, and offers theoretical insights for microbe-base targeted restoration practices.

Materials and Methods

Study Area and Experimental Design

The study was conducted in August 2023 (late growing season) on representative riverbank sand mining sites along the south bank of the upper Huai River (114°04′27″-114°04′46″ E, 32°21′12″-32°21′27″ N) (Fig. 1). The study area is located in a climatic transition zone between the subtropical and warm temperate regions, characterized by a mean annual temperature of 15.3-15.8°C, mean annual precipitation of 993-1294 mm (30-year normal for 1991-2020 from the China Surface Climate Normals Dataset, developed by the National Meteorological Information Centre of CMA; Zhao et al. 2024, based on daily observations at Xinyang Station, Station ID:57297, follow WMO guidelines), and mean annual relative humidity of 74-78%. The sites have undergone natural recovery since 2017. The soil is highly sandy with generally flat terrain. Due to local spatial heterogeneity in soil nutrients, the vegetation exhibits a patchy distribution, with dominant pioneer species including *Artemisia scoparia* (As), *Saccharum arundinaceum* (Sa), *Imperata cylindrica* (Ic), and scattered solitary trees (St). Based on vegetation type and patch distribution, four spatially replicated plots were established for each vegetation type, resulting in a total of 16 plots. The distance between adjacent plots exceeded 50 m to minimize mutual interference.

Soil Sample Collection

Soil sampling methods followed those described in our previous study (Qin et al. 2026). For plots dominated by *A. scoparia* and *I. cylindrica*, 1 m × 1 m quadrats were established, and soil samples were collected from depths of 0-20 cm and 20-40 cm using a five-point sampling method. In *S. arundinaceum* plots, 5 m × 5 m quadrats were established, and soil profiles were excavated at the base of four corner plants and one central plant to collect samples from 0-20 cm and 20-40 cm depths. For solitary tree plots, soil profiles were excavated at the base of each tree trunk to collect samples from the same depth intervals. Within each plot, soil samples from the same layer were homogenized to form a single composite sample, yielding a total of 32 soil samples (4 vegetation types × 4 replicates × 2 soil layers). Each composite sample was divided into two subsamples: one fresh subsample was preserved in an ice box, immediately transported to the laboratory, and stored at -80°C for microbial analysis; the other subsample was air-dried, passed through a 2 mm sieve, and stored at 4°C for determination of soil nutrient contents and enzyme activities. Additionally, undisturbed soil cores were collected using the cutting ring method for analysis of soil physical properties. Concurrently, aboveground plant tissues were collected from all plots for analysis of plant nutritional traits (data not shown in this study; see Qin et al. 2026). The three plant species, *A. scoparia*, S*. arundinaceum* and *I. cylindrica*, were collected directly from the riparian sand mining sites located in Shihe District, Xinyang city,

Henan Province, China. No plant material was obtained from institutional or commercial source.

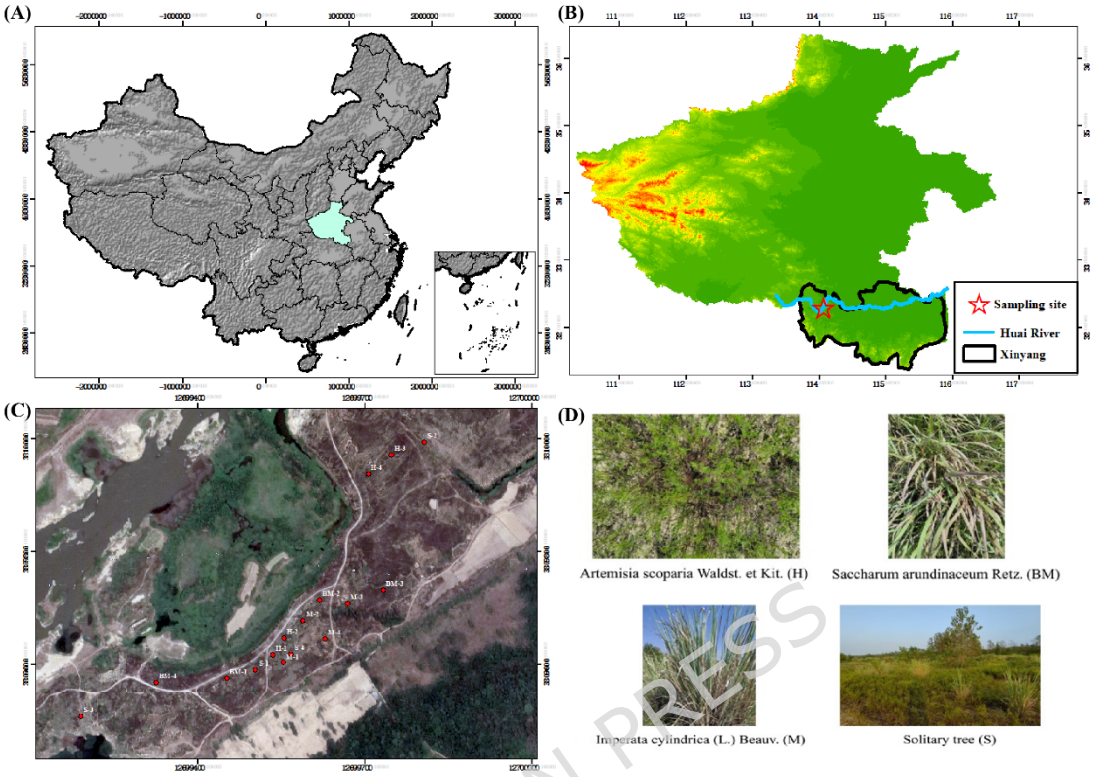

Fig. 1 The sampling area is located in Huai River riparian buffer zone (C), Henan province (B), China (A). The map was generated using ArcGIS Desktop version 10.8 (Esri, Redlands, CA, USA; https://www.esri.com) based on standard basemap layers.

Analysis of Soil Physicochemical Properties, Enzyme Activities, and Plant Nutritional Traits

The measured parameters were categorized as follows. Soil physical properties included bulk density (BD), soil water content (SWC), total soil water holding capacity (TSWC), field soil water holding capacity (FSWC), total porosity (TPR), capillary porosity (CP), and non-capillary porosity (NCP). Soil chemical properties included pH, soil total carbon (TC), soil total nitrogen (TN), soil total phosphorus (TP), available phosphorus (AP), ammonium nitrogen (NH_4-N), and nitrate nitrogen (NO_3-N). Particle size fraction carbon distribution was characterized as coarse sand-sized organic carbon (TC3), fine sand-sized organic carbon (TC2), and silt+clay-sized organic carbon (TC1). Soil enzyme activities analyzed were sucrase (SUC), protease (Prot), and urease (URE). Vegetation nutritional traits included plant total carbon (PlantC), plant total nitrogen (PlantN), and plant total phosphorus (PlantP). Detailed analytical methods for all parameters are described in Qin et al. (2026).

Key Soil Environmental Indicators Selection and Multifunctionality Index Calculation

To avoid multicollinearity and identify the core environmental factors driving microbial community dynamics, Pearson correlation analysis was performed on all measured soil physicochemical and biochemical parameters, and variance inflation factors (VIFs) were calculated. Based on ecological representativeness and an iterative elimination procedure (removing variables with VIF > 10), 12 key indicators were ultimately retained for subsequent analyses: BD, SWC, CP, TC, TP, TN, AP, NH_4^+-N, NO_3^--N, URE, Prot, and TC1.

Based on these 12 selected indicators, we evaluated four functional aspects related to soil environmental improvement capacity across different vegetation types in the sand mining sites: physical condition improvement capacity (BD, SWC, CP), carbon storage capacity (TC, TC1, URE), nitrogen supply capacity (TN, NH_4^+-N, NO_3^--N, Prot), and phosphorus supply capacity (TP, AP). These selected functions and characteristics are generally consistent with those employed in previous multifunctionality studies (Chen et al., 2023; Ying et al., 2023). We assumed that increases in all indicator values were desirable, with the exception of BD. Prior to calculating soil multifunctionality, all parameters were Z-score standardized. BD values were multiplied by -1 to ensure directional consistency with other indicators (i.e., lower BD is considered beneficial). Subsequently, we constructed soil multifunctionality indices using three approaches: the mean method, a PCA-based approach, and a multiple threshold approach, all of which have been widely applied in soil multifunctionality research (Byrnes et al., 2014). To ensure the representativeness of the final composite index, correlation analysis revealed that the indices derived from the three methods were highly correlated ($r > 0.929$), indicating strong consistency in multifunctionality ranking among samples (Fig. S1). The mean method was selected as the final soil multifunctionality index due to its transparent calculation process, intuitive ecological interpretability, and the continuous nature of the resulting variable, which is most suitable for subsequent statistical analyses and complex modeling.

Soil Microbial Community Analysis

Genomic DNA was isolated from 0.5 g of each homogenized soil sample (n = 36) using the PowerSoil DNA Isolation Kit (Mo Bio Laboratories, Solana Beach, CA, USA) according to the manufacturer's instructions. The V3-V4 hypervariable regions of the bacterial 16S rRNA gene were amplified using primers 338F/806R, and the fungal ITS1 region was amplified using primers ITS1F/ITS2R (Guo et al., 2022; Yu et al., 2024). PCR amplification was performed in a 25 μL reaction mixture containing 12.5 μL of ABI Power SybrGreen qPCR Master Mix (Applied Biosystems), 0.5 μM of each primer, 1 μL of template DNA (20 ng μL^{-1}), and sterile distilled water. The thermal cycling conditions consisted of an initial denaturation at 95°C for 1 min, followed by 30 cycles of 95°C for 15 s, 55°C for 30 s, and 72°C for 30 s. PCR products were extracted from 2% agarose gels, purified using an AxyPrep DNA Gel Extraction Kit (Axygen Biosciences, Union City, CA, USA), and quantified using a QuantiFluor™-ST fluorometer (Promega, Madison, WI, USA). The purified amplicons were paired-end sequenced (2 × 300 bp) on an Illumina MiSeq platform by Origingene Biotechnology Co., Ltd. (Shanghai, China).

Raw sequencing data were processed using the QIIME2 pipeline (version 2024.10). Primer sequences were trimmed using the cutadapt plugin. Subsequently, quality filtering, denoising, read merging, and chimera removal were performed using the DADA2 plugin to generate amplicon sequence variants (ASVs) based on a 99% similarity threshold. A total of 1,621,058 high-quality bacterial sequences and 2,267,012 high-quality fungal sequences were obtained. To ensure equal sequencing depth for downstream diversity comparisons, all samples were rarefied to the minimum sequence count across samples (30,000 sequences per sample for bacteria; 28,000 sequences per sample for fungi). Taxonomic assignment of bacterial ASVs was performed against the SILVA 138.1 database (release data: 27 August 2020; accessed 15 March 2024), while fungal ASVs were annotated using the UNITE 8.0 database (release data: 2019; accessed 18 March 2024). The raw sequence reads have been deposited in the National Microbiology Data Center (NMDC) under accession number NMDC10020688. The data can be accessed directly at https://nmdc.cn/resource/genomics/project/detail/NMDC10020688. Other datasets generated and/or analysis during the current study (e.g., plant nutrient, soil properties) are available from the corresponding author upon reasonable request.

Statistical Analysis, Network Construction, and Functional Prediction

All statistical analyses were performed using R software (version 4.2.0). Prior to group comparisons, all continuous variables were tested for normality (Shapiro-Wilk test) and homogeneity of variance (Levene's test). Data that did not meet the assumptions of parametric tests were appropriately transformed using logarithmic or square-root transformations. Two-way ANOVA was employed to examine the effects of vegetation type and soil depth on microbial alpha diversity, while one-way ANOVA followed by Tukey's HSD post-hoc test was used to compare soil multifunctionality and βNTI among vegetation types. For comparisons of microbial taxon abundances and functional prediction abundances between two groups, Wilcoxon rank-sum tests were performed, and *p*-values were adjusted for false discovery rate (FDR) using the Benjamini-Hochberg (BH) method to control for Type I errors due to multiple comparisons.

Permutational multivariate analysis of variance (PERMANOVA) and Permutational Analysis of Multivariate Dispersions (PERMDISP) based on the Bray-Curist distance matrix was conducted using the *vegan* package to test for differences in microbial community structure among vegetation types and within groups, respectively. Redundancy analysis (RDA) was performed to identify and quantify the key environmental factors driving community composition. To avoid model overfitting and multicollinearity, forward selection was applied using the *ordiR2step* function (vegan package) with the Akaike information criterion (AIC) to select a minimal set of environmental variables that significantly contributed to explaining community variation. A final RDA model was then constructed based on the selected variable set. To evaluate the independent contribution and significance of each key environmental factor in the final RDA model, the *rdacca.hp* package was used to calculate conditional effects, thereby quantifying the proportion of community variation uniquely explained by each factor along with its statistical significance (based on 999 permutations) (Lai et al. 2022). To further explore the specific associations between different types of environmental factors and key microbial taxa, Mantel tests were performed. Environmental factors were categorized into four groups: soil physical properties (BD, SWC, CP), soil chemical properties (TC, TN, TP, AP, NH_4-N, NO_3-N), soil enzyme activities (URE, Prot), and plant nutritional traits (PlantN, PlantP). For microbial communities, the top 10 most abundant phyla (at the phylum level) for both bacteria and fungi were extracted, and distance matrices were constructed based on their abundance data. The Mantel correlation coefficient (*r*) and its significance (999 permutations) between each environmental factor group matrix and the bacterial or fungal key taxon abundance matrix were calculated using the linkET package, thereby assessing the overall influence of various environmental pressures on the distribution of dominant microbial taxa.

Microbial Co-occurrence Network Construction and Stability Analysis

Microbial co-occurrence networks for bacteria and fungi were constructed separately for each vegetation type based on Spearman correlation coefficients. Only correlations with $|r| > 0.6$ and FDR-corrected $p < 0.05$ were retained for network construction. Network visualization was performed using Gephi software. Network topological properties, including average clustering coefficient (avgCC), average path length (APD), graph density (GD), and modularity (M), were calculated using the igraph package. Additionally, keystone taxa were identified by calculating within-module connectivity (Z_i) and among-module connectivity (P_i) for each node. Following the criteria of Ge et al. (2025) and Deng et al. (2012), nodes were classified as network hubs ($Z_i > 2.5$ and $P_i > 0.62$), module hubs ($Z_i > 2.5$ and $P_i < 0.62$), or connectors ($Z_i < 2.5$ and $P_i > 0.62$). All these categories are collectively referred to as keystone taxa. To quantify microbial network stability, positive cohesion and negative cohesion were calculated following the framework proposed by Herren and McMahon (2017). This method assesses the potential strength of cooperative (positive cohesion) and competitive (negative cohesion)

interactions by summing the weighted positive and negative correlations between each pair of species within the community.

Prediction of Microbial Ecological Functions and Resource Utilization Potential

Functional annotation of bacterial ASVs was performed using the FAPROTAX database to predict their potential roles in biogeochemical cycles, including carbon, nitrogen, and sulfur cycling. Fungal ASVs were assigned to functional guilds using the FUNGuild database, classifying them into trophic modes such as saprotrophs, symbiotrophs, and pathotrophs (Qiu et al. 2025). To assess the resource utilization capacity of soil microbial communities under different vegetation types, Levins' niche breadth index was calculated based on ASV-level relative abundance data using the formula $B = 1/\sum(P_i^2)$, where P_i represents the relative abundance of species *i*. A higher index value indicates a broader resource utilization spectrum and a wider ecological niche (Qiu et al. 2023).

Community Assembly Processes and Structural Equation Modeling

To quantify the relative contributions of deterministic and stochastic processes in community assembly, null model analysis based on phylogenetic β diversity was performed. The beta nearest taxon index (βNTI) was calculated for each pair of samples. $|\beta\text{NTI}| > 2$ indicates dominance by deterministic processes (homogeneous selection or variable selection), whereas $|\beta\text{NTI}| < 2$ suggests dominance by stochastic processes (dispersal limitation or homogenizing dispersal). iCAMP (phylogenetic-bin-based null model analysis) was used to quantify assembly processes. Rather than applying null model to the entire community, iCAMP first partitions all taxa into phylogenetic “bins” based on a phylogenetic signal threshold ($d_S = 0.2$), within which the phylogenetic signal of microbial niche preference is generally found significant across various environments. Assembly processes are then quantified separately within each bin using βNTI and modified Raup-Crick (RC) metrics, and bin-level results are aggregated by abundance weighting. This binning strategy provides robustness to low or medium phylogenetic signal across the full phylogency, as iCAMP maintains high accuracy (0.93-0.99) and precision (0.80-0.94) even under low-signal scenarios (Ning et al. 2020). Specifically: $\beta\text{NTI} < -2$ indicates community assembly dominated by homogeneous selection; $\beta\text{NTI} > 2$ indicates assembly dominated by variable selection; $|\beta\text{NTI}| < 2$ and $RC > 0.95$ indicates assembly dominated by dispersal limitation; $|\beta\text{NTI}| < 2$ and $RC < -0.95$ indicates assembly dominated by homogenizing dispersal; and $|\beta\text{NTI}| < 2$ with $|RC| < 0.95$ indicates assembly governed by undominated processes (e.g., weak selection or dispersal) (Barnett et al. 2020; Peng et al. 2025).

To elucidate the causal network relationships among vegetation type, soil environment, microbial community, and soil multifunctionality, partial least squares structural equation modeling (PLS-SEM) was conducted. We hypothesized that vegetation type affects soil multifunctionality indirectly, first by modifying soil physical and chemical properties, which then influence microbial community diversity and composition.The following constructs were included: vegetation type (PlantN, PlantP), soil physical properties (BD, SWC, Hpro), soil chemical properties (TC, TP, TN, AP, NH_4^+-N, NO_3^--N, TC1), microbial α diversity (Richness, Shannon index, Chao1 index, PD_whole_tree), microbial β diversity (PCoA1 and PCoA2 scores derived from principal coordinate analysis based on bacterial and fungal Bray-Curtis distance matrices), and soil multifunctionality (mean-based soil multifunctionality index calculated in Section 2.4). Prior to constructing latent variables, all measured variables were Z-score standardized. For latent variables comprising multiple indicators, principal component analysis was first performed, ensuring that the first principal component (PC1) explained more than 80% of the variance, thereby effectively representing the original information. Separate PLS-SEM models were constructed for bacterial and fungal communities. Model fitting was performed using the plspm package in R. The measurement model was first evaluated by examining factor loadings of observed variables on their respective latent

constructs (> 0.7), and construct reliability and convergent validity were assessed using composite reliability (CR > 0.7) and average variance extracted (AVE > 0.5). For the structural model, bootstrap resampling (999 iterations) was used to test the significance of path coefficients ($p < 0.05$). The explanatory power of the model for endogenous variables was evaluated using the coefficient of determination (R^2), while fit quality was assessed using the global goodness-of-fit (GOF) index.

No custom scripts or bespoke computational codes were generated for this study. All statistical analyses and visualizations were performed using publicly available R packages (version 4.2.0) and other standard software as detailed in the Methods section.

Results

Variations in Soil Multifunctionality Indicators Across Different Pioneer Vegetation Types in Riparian Sand Mining Sites

Soil multifunctionality indicators varied considerably among the different pioneer vegetation types. *Artemisia scoparia* communities were characterized by higher NH_4-N and Prot contents. *Saccharum arundinaceum* communities exhibited higher SWC and lower BD. *Imperata cylindrica* communities showed higher soil TC, TN, TP, AP, and NO_3-N contents. Solitary tree plots were characterized by higher CP, TC1, and URE (Fig. 2A). Overall, soil multifunctionality was highest in *I. cylindrica* communities, which was significantly higher than that in *A. scoparia* communities (Fig. 2B).

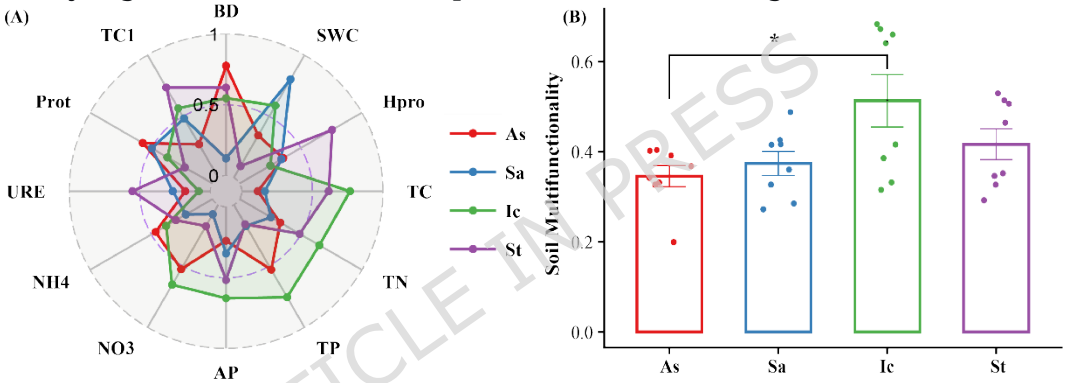

Fig. 2 Spider plot (A) and bar chart (B) of soil multifunctionality under different pioneer vegetation types in riparian sand mining sites. Asterisks (*) indicate significant differences between groups ($p < 0.05$). As: *A. scoparia*; Sa: *S. arundinaceum*; Ic: *I. cylindrica*; St: solitary trees.

Soil Microbial Community Structure and Diversity Under Different Pioneer Vegetation Types

Although soil microbial α diversity did not exhibit significant differences among vegetation types (while Richness, Chao1, PD_whole_tree of bacterial communities in solitary tree plots were significantly higher in the deeper layer than surface layer) (Fig. S1, Fig. S2), community composition showed a clear response to vegetation type. Redundancy analysis (RDA) revealed that bacterial community structure differed significantly among vegetation types (PERMANOVA, $p < 0.001$; PERMDISP, $p < 0.001$), with the first axis explaining 43.16% of the variation. *I. cylindrica* and *S. arundinaceum* communities were positioned on opposite sides of the first axis. The second axis explained 33.64% of the variation, with *A. scoparia* communities distributed on the upper side and other communities on the lower side (Fig 3A). Analysis of key environmental factors indicated that TC, TP, and NO_3-N were the primary drivers of bacterial community differentiation, explaining 29.43%, 25.62%, and 22.78% of the community variation, respectively (Fig. 3B). In contrast, fungal community composition did not differ significantly among vegetation types (PERMANOVA, p = 0.172), and within-group dispersion was also not significantly heterogeneous (PERMDISP, p = 0.632). RDA results showed that the first and second axes explained 36.79% and 33.64% of the variation,

respectively. *I. cylindrica* and *S. arundinaceum* communities were distributed on opposite sides of the first axis, while the distribution of communities along the second axis showed no clear separation among vegetation types (Fig 3C). Prot, TC, and TP were identified as the main factors influencing fungal community distribution, explaining 48.45%, 26.55%, and 25.18% of the community variation, respectively (Fig 3D).

At the phylum level, the soil bacterial communities across different pioneer vegetation types in the riparian sand mining sites were predominantly composed of *Proteobacteria* (15.9-36.4%), *Actinobacteriota* (9.2-31.48%), *Acidobacteriota* (9.8-49.8%), and *Chloroflexi* (3.9-22.9%) (Fig 4, A). Among these, *A. scoparia* communities exhibited the highest relative abundance of *Actinobacteriota*, which was significantly greater than the other vegetation types. Solitary tree plots showed the highest abundances of *Bacteroidota* and *Firmicutes*, significantly exceeding other vegetation types. *I. cylindrica* communities had the highest abundances of *Nitrospirota* and *Patescibacteria*, which were significantly higher than the other vegetation types (Fig. 4SA).

The soil fungal communities were primarily composed of *Ascomycota* (9.7-63.2%), *Unclassified Fungi* (5.4-58.9%), *Basidiomycota* (1.0-77.2%), and *Fungi_phy_Incertae_sedis* (1.5-37.1%) (Fig. 4B). Solitary tree plots exhibited the highest relative abundance of *Basidiomycota*, which was significantly greater than *A. scoparia* and *S. arundinaceum* communities (Fig. S4B).

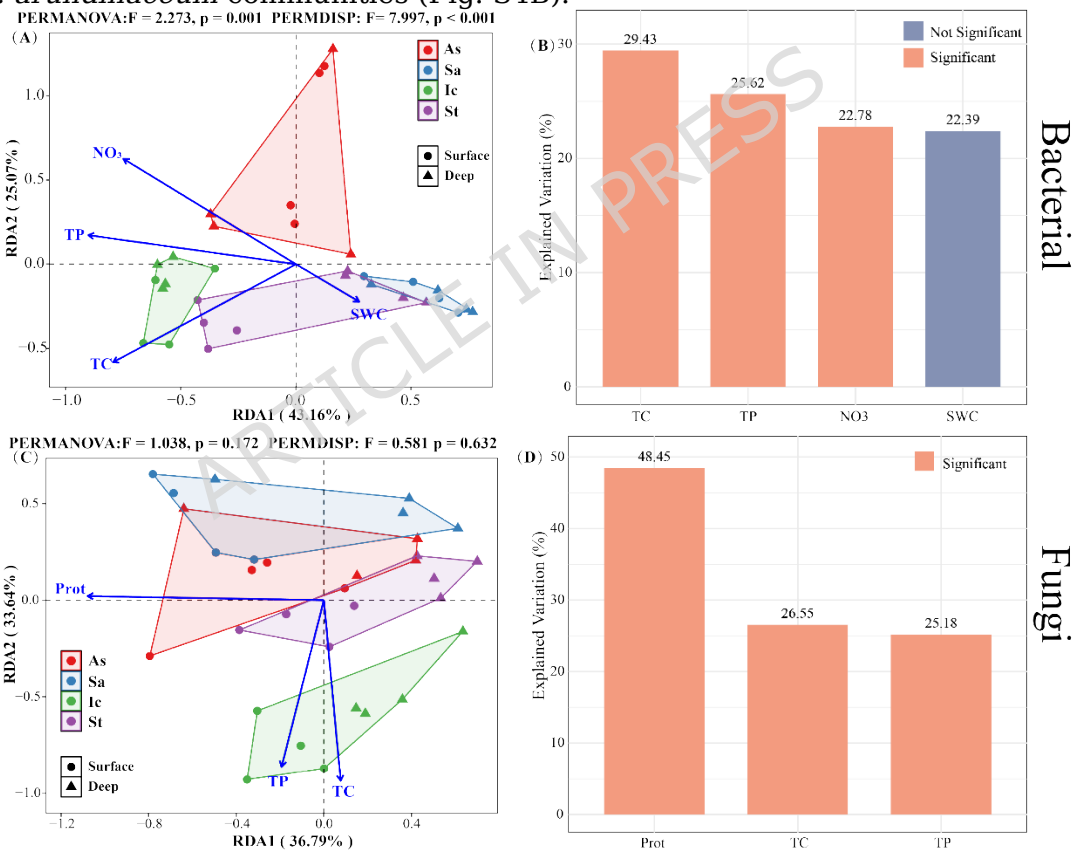

Fig. 3 Distribution characteristics of soil microbial communities under different pioneer vegetation types in riparian sand mining sites. Redundancy analysis (RDA) showed the effects of soil physicochemical properties on bacterial communities in the riparian sand mining sites (A), and variation partitioning analysis (VPA) revealed the explained proportions and significance of soil physicochemical properties in shaping bacterial communities (B); Redundancy analysis (RDA) showed the effects of soil physicochemical properties on fungal communities in the riparian sand mining sites

(C), and variation partitioning analysis (VPA) revealed the explained proportions and significance of soil physicochemical properties in shaping fungal communities (D). As: *A. scoparia*; Sa: *S. arundinaceum*; Ic: *I. cylindrica*; St: solitary trees.

Influence of Environmental Factors on Microbial Communities

Mantel tests revealed significant associations between soil properties and specific microbial taxa (Fig. 5). Soil physical properties were significantly correlated with *Myxococcota* ($0.01 < p < 0.05$) and *Chytridiomycota* ($p < 0.01$). Soil chemical properties showed significant correlations with *Acidobacteriota* ($0.01 < p < 0.05$) and *Actinobacteriota* ($p < 0.01$). Soil enzyme activities were significantly correlated with *Mortierellomycota* ($p < 0.01$).

Further analysis of the relationships between different category of soil physicochemical factors and microbial community diversity, revealed that bacterial diversity was significantly negatively correlated with TP and NO_3-N, whereas fungal diversity showed a significant positive correlation with TC (Fig. 3S).

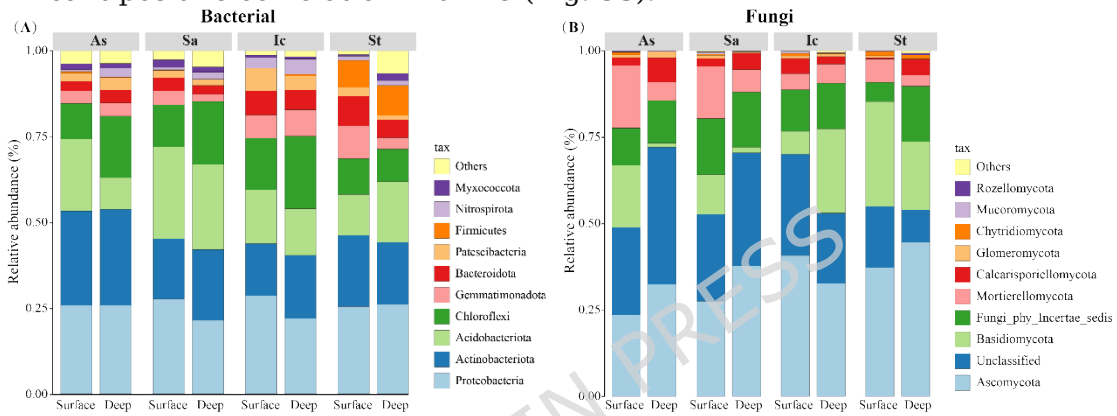

Fig. 4 Bacterial (A) and fungal (B) community composition at the phylum level under different pioneer vegetation types in riparian sand mining sites. As: *A. scoparia*; Sa: *S. arundinaceum*; Ic: *I. cylindrica*; St: solitary trees.

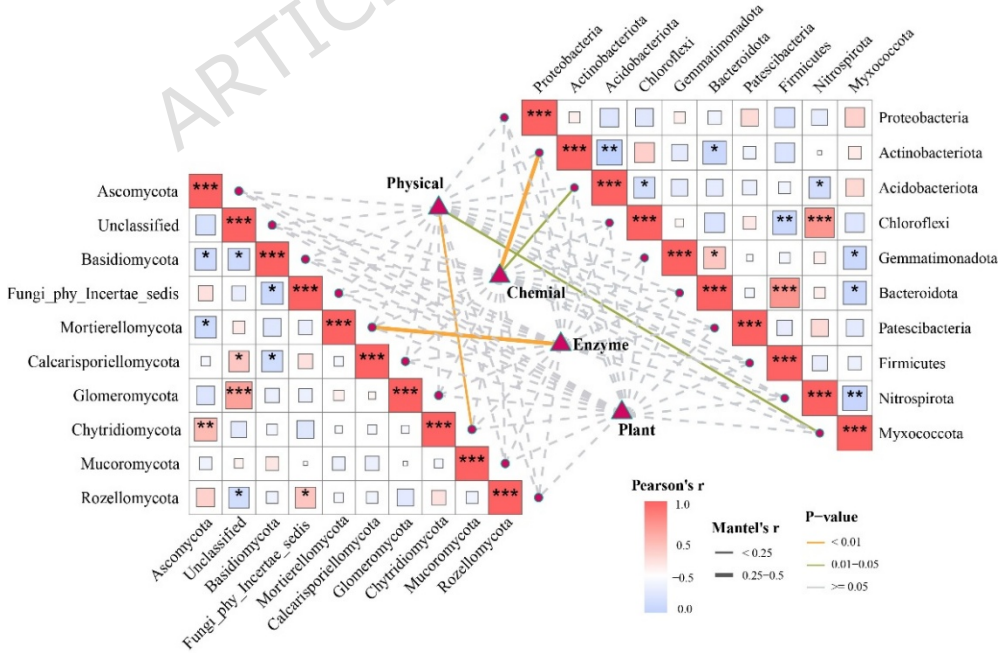

Fig. 5 Butterfly diagram illustrating the correlation between soil functional profile and microbial top10 taxies at phylum level. Solid line connections indicate significant

Mantel test results, with edge width proportional to the Mantel r statistic and color denoting significance level (blue: p < 0.01; green: $p < 0.05$); (Left) Heatmap of pairwise spearman correlations among fungal community taxa. (Right) Heatmap of pairwise spearman correlations among bacterial community taxa. (* indicated significance at the 0.05 level; ** indicated significance at the 0.01 level, *** indicated significance at the 0.001 level).

Microbial Co-occurrence Network Structure and Stability

The co-occurrence networks of microbial communities under different pioneer vegetation types in the riparian zone were predominantly characterized by positive connections. The proportion of negative correlations was generally higher in bacterial networks than in fungal networks, particularly in *A. scoparia* plots. Analysis of network topological properties revealed that the bacterial network in solitary tree plots was the most complex (nodes = 217, edges = 941), whereas that in *I. cylindrica* plots was the simplest (nodes = 150, edges = 231). Fungal network complexity showed relatively minor differences among vegetation types; however, *I. cylindrica* and *S. arundinaceum* plots exhibited a greater number of edges (Table 1).

All networks exhibited high average clustering coefficients (avgCC > 0.5) and modularity values, consistent with the characteristics of “small-world” networks (Fig. 6). Notably, fungal networks generally displayed higher avgCC values than bacterial networks. Average path lengths (APD) were generally between 4 and 6, facilitating rapid transmission of information or disturbances within the networks. Relatively lower APD values were observed in the bacterial network of *I. cylindrica* and the fungal network of *S. arundinaceum*. Graph density was consistently low (< 0.04) across all networks; however, the bacterial network in solitary tree plots showed a relatively higher GD value (Table 1).

Identification of Keystone Microbial Taxa and Functional Prediction

Zi-*Pi* analysis identified keystone microbial taxa within the soil microbial networks under different pioneer vegetation types (Fig. 5S). Bacterial keystone taxa were generally more numerous and phylogenetically diverse than fungal keystone taxa, with their composition exhibiting pronounced vegetation specificity. In *A. scoparia* communities, keystone taxa primarily belonged to the phyla *Alphaproteobacteria*, *Acidobacteriota*, and *Verrucomicrobiota*, with particular attention to *Defluviicoccaceae* and *Myxococcota*. In *S. arundinaceum* communities, keystone taxa were mainly affiliated with *Alphaproteobacteria*, *Gammaproteobacteria*, *Acidobacteriota*, *Chloroflexi*, and *Verrucomicrobiota*. In *I. cylindrica* communities, keystone taxa predominantly belonged to *Actinobacteriota* and *Acidobacteriota*, including *Iamiaceae* and multiple *Acidobacteriota* subgroups. In solitary tree plots, keystone taxa exhibited the broadest phylogenetic diversity, encompassing *GAL15*, *Gammaproteobacteria*, *Desulfobacterota*, *Acidobacteriota*, *Verrucomicrobiota*, and other lineages (Table 1S).

Compared with bacteria, fungal keystone taxa showed more pronounced variation among vegetation types. In *A. scoparia* plots, five fungal keystone taxa were detected, of which four belonged to *Ascomycota* and one to *Glomeromycota*. In *I. cylindrica* communities, four keystone taxa were identified, including three from *Basidiomycota* and one from *Chytridiomycota*. In solitary tree plots, five keystone taxa were identified, with three belonging to *Ascomycota* and the remaining two to *Basidiomycota* and *Chytridiomycota*, respectively. Notably, no fungal keystone taxa meeting the threshold criteria were detected in *S. arundinaceum* communities (Table 1S).

It is important to note that FAPROTAX and FUNGuild predict potential metabolic or trophic functions based on taxonomic annotation, not directly measured process rates. The results presented here therefore reflect functional potential rather than in situ fluxes. FAPROTAX revealed that the relative abundance of *aerobic ammonia oxidation* and *nitrification* function predicted was significantly lower in *I. cylindrica* than in other vegetation types. The function potential of soil bacterial communities in the riparian

sand mining sites under different pioneer vegetation types was predominantly associated with nitrogen cycling processes. Specifically, *I. cylindrica* exhibited significantly lower abundances of *aerobic ammonia oxidation* and *nitrification* function predicted compared to other vegetation types, while solitary tree plots and *I. cylindrica* showed significantly higher potentials for *nitrate denitrification* and *nitrite denitrification*. Fungal community functions were predominantly characterized by *litter saprotrophs*, with no significant differences among vegetation types; however, a strong *ectomycorrhizal* signal was detected exclusively in solitary tree plots (Fig. 6S).

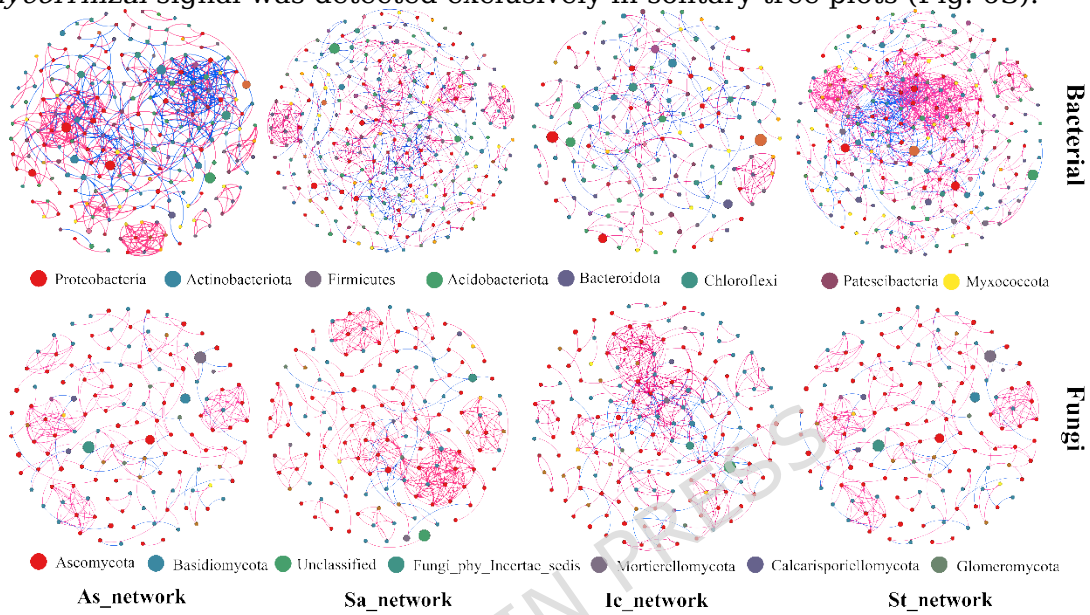

Fig. 6 Co-occurrence networks of the soil microbial community under different pioneer vegetation types in riparian sand mining sites. The colors assigned to nodes and edges in the networks indicate different major phyla and the types of interactions, respectively. Red, positive links; Blue, negative links. As: *A. scoparia*; Sa: *S. arundinaceum*; Ic: *I. cylindrica*; St: solitary trees.

Table 1 Topological properties of the co-occurrence networks of microbial communities under different pioneer vegetation types in riparian sand-mining sites. As: *A. scoparia*; Sa: *S. arundinaceum*; Ic: *I. cylindrica*; St: solitary trees.

	Network parameter	***As***	***Sa***	***Ic***	***St***
Bacterial	Node	216	228	150	217
	Edge	659	576	231	941
	Positive	431	401	148	744
	Negative	228	175	83	197
	avgCC	0.536	0.585	0.515	0.598
	APD	4.882	5.163	4.470	4.727
	GD	0.028	0.022	0.021	0.040
	M	0.700	0.746	0.818	0.514

Fungi	Node	137	141	154	148
	Edge	263	372	373	310
	Positive	236	340	304	265
	Negative	27	32	69	45
	avgCC	0.771	0.756	0.581	0.617
	APD	5.800	4.527	5.141	5.427
	GD	0.028	0.038	0.032	0.028
	M	0.848	0.749	0.660	0.828

avgCC, clustering coefficient; APD, average path distance; GD, graph density; M, modularity.

Microbial Community Assembly Processes and Network Stability

Based on null model analysis (*β*NTI), the assembly processes of soil microbial communities differed significantly among pioneer vegetation types in the riparian sand mining sites. For bacterial communities, *β*NTI values < -2 in *A. scoparia* and *S. arundinaceum* plots indicated dominance by deterministic processes. In contrast, *β*NTI values between -2 and 2 in solitary tree and *I. cylindrica* plots suggested stochastic processes predominated. Notably, *β*NTI in solitary tree plots was significantly higher than in the other three vegetation types (Fig. 7A). Specifically, bacterial community assembly in *A. scoparia* and *S. arundinaceum* was primarily driven by homogeneous selection. In *I. cylindrica* communities, the contribution of homogeneous selection decreased, with dispersal limitation becoming the dominant process. In solitary tree plots, community assembly was jointly influenced by variable selection and dispersal limitation (Fig. 7C).

For fungal communities, assembly processes in *S. arundinaceum* plots were dominated by deterministic processes, whereas communities in the other three vegetation types were primarily governed by stochastic processes. Solitary tree plots exhibited the highest *β*NTI values, significantly greater than the other vegetation types, followed by *S. arundinaceum* plots, which were significantly higher than those in *A. scoparia* plots (Fig. 7B). Fungal community assembly in *A. scoparia*, *S. arundinaceum*, and *I. cylindrica* was mainly attributed to dispersal limitation and homogeneous selection, with homogeneous selection contributing slightly more than dispersal limitation in *S. arundinaceum* plots. In solitary tree plots, dispersal limitation was the predominant process governing fungal community assembly (Fig. 7D).

Network stability of soil microbial communities under different pioneer vegetation types was assessed using cohesion analysis. Bacterial network stability exhibited pronounced vegetation specificity. *S. arundinaceum* bacterial communities showed the highest positive cohesion and the lowest absolute negative cohesion. Conversely, solitary tree bacterial communities exhibited the lowest positive cohesion, while *I. cylindrica* bacterial communities displayed the highest absolute negative cohesion (Fig 8. A, D); The stability patterns of fungal networks differed from those of bacterial networks. *I. cylindrica* fungal communities exhibited significantly higher positive and negative cohesion than other vegetation types. In contrast, *A. scoparia* fungal networks showed the lowest levels of both positive and negative cohesion (Fig. 8 B, E).

Resource utilization capacity of soil microbial communities under different pioneer vegetation types was further evaluated through niche breadth analysis. Bacterial communities in *I. cylindrica* plots exhibited significantly broader niche breadth than those in other vegetation types. No significant differences in fungal community niche breadth were observed among vegetation types (Fig. 8 C, F).

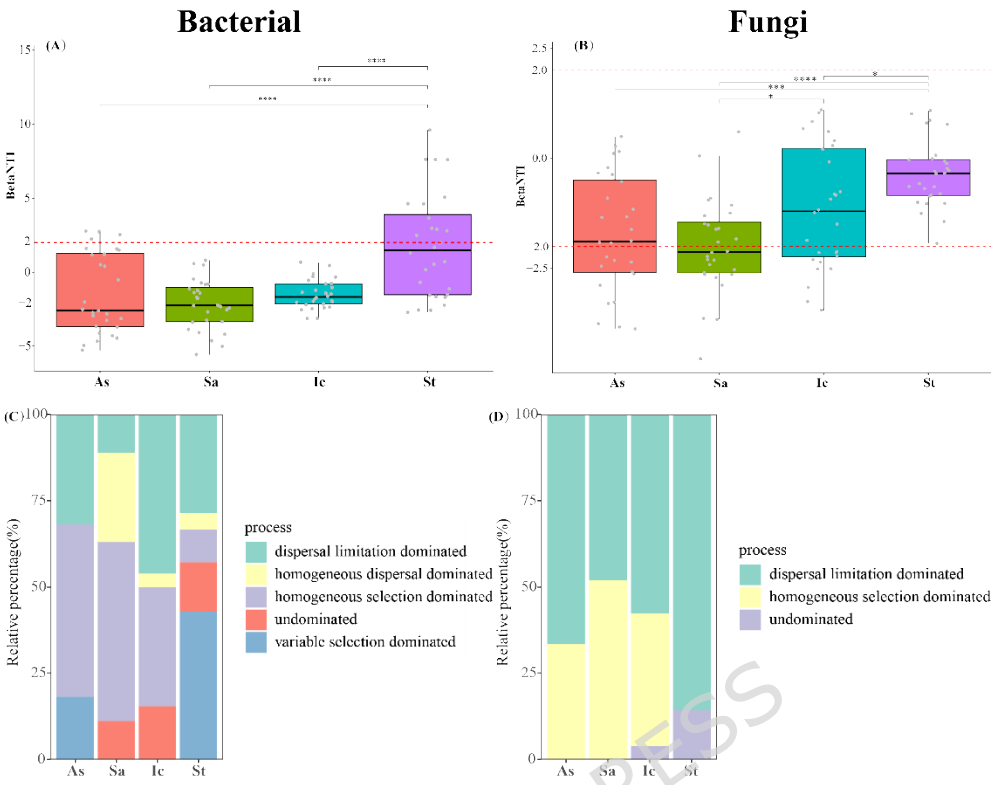

Fig. 7 Community assembly mechanisms of soil bacteria and fungi under different pioneer vegetation types in riparian sand mining sites. (A, B) βNTI values indicating the balance between deterministic and stochastic processes; (C, D) Relative contributions of specific ecological processes. As: *A. scoparia*; Sa: *S. arundinaceum*; Ic: *I. cylindrica*; St: solitary trees.

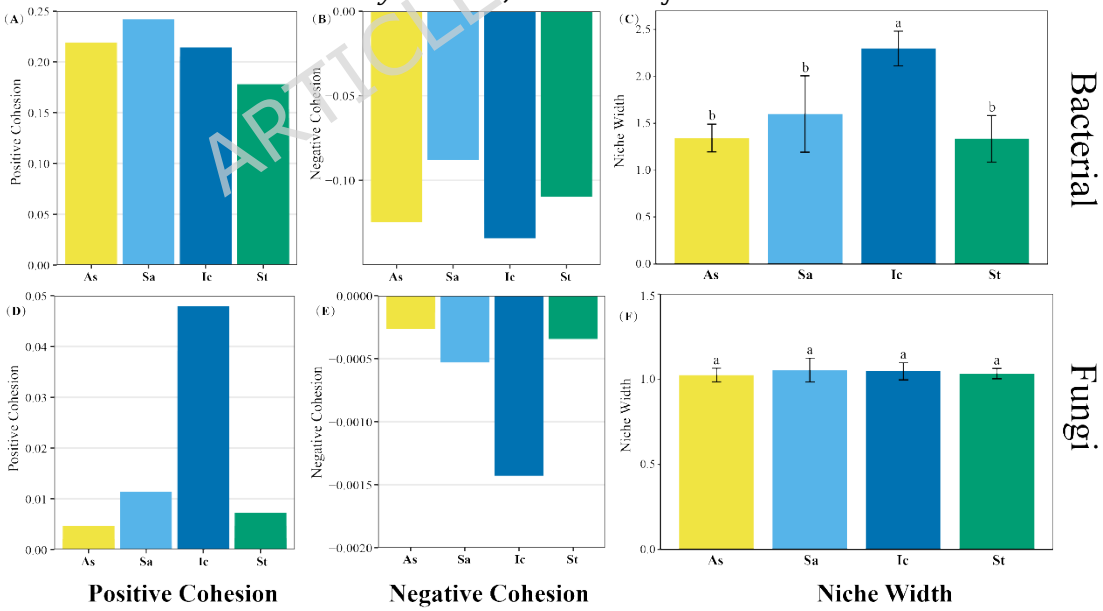

Fig. 8 Comparison of cohesion indices and niche breadth between bacterial and fungal communities under different pioneer vegetation types in riparian sand mining sites. (A, D) Positive cohesion; (B, E) Negative cohesion; (C, F) Niche breadth. Data are shown as mean ± SE. Different letters indicate significant differences among vegetation types ($p < 0.05$). As: *A. scoparia*; Sa: *S. arundinaceum*; Ic: *I. cylindrica*; St: solitary trees.

Regulation of Soil Multifunctionality by the Vegetation–Soil–Microbe Continuum

Structural equation modeling revealed the indirect pathways through which vegetation type influences soil multifunctionality (Fig. 9). The results indicated that microbial community composition and diversity exerted no direct effects on soil multifunctionality; instead, soil physical properties played a crucial mediating role. Vegetation type indirectly regulated soil multifunctionality through soil physical properties; however, this pathway exhibited opposite directions in the bacterial and fungal models. In the bacterial model, vegetation type showed a positive effect on soil physical properties, while soil physical properties exerted a negative effect on multifunctionality. In contrast, in the fungal model, vegetation type demonstrated a negative effect on soil physical properties, whereas soil physical properties had a positive effect on multifunctionality.

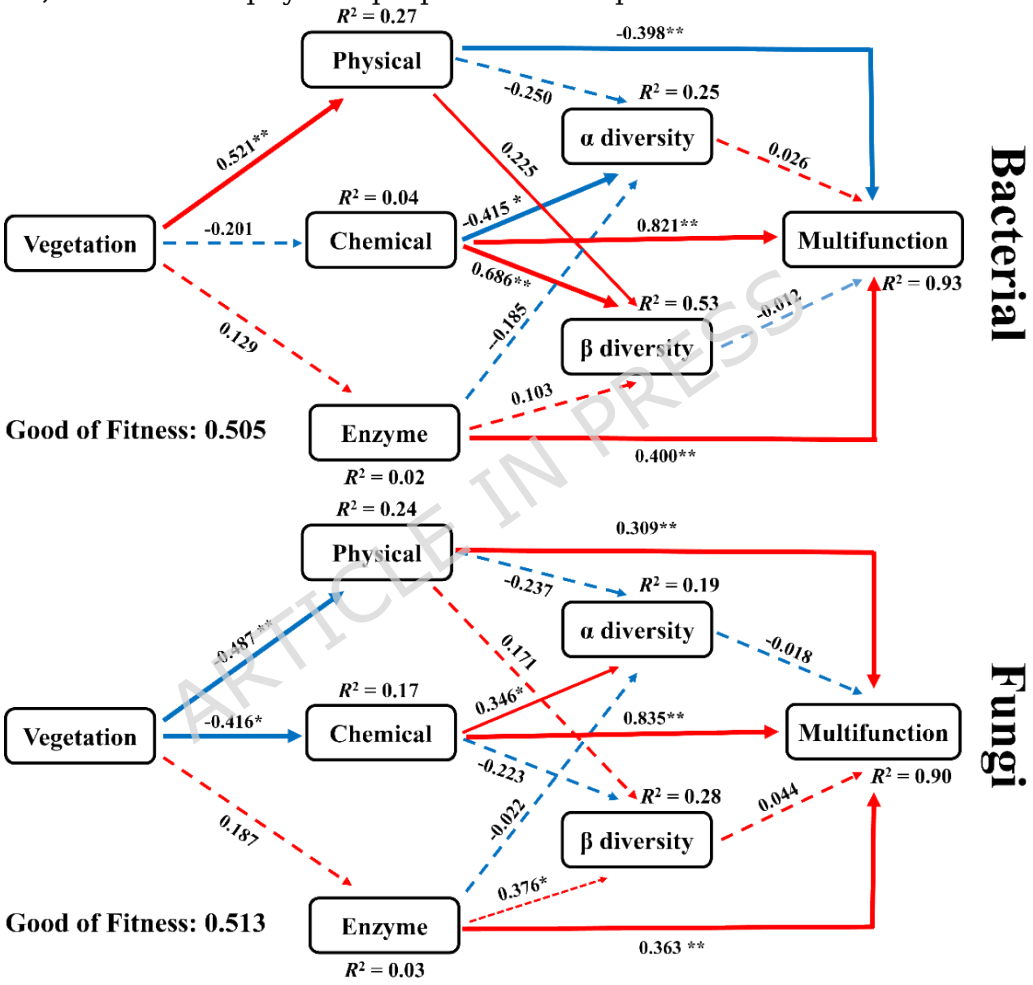

Fig. 9 The Partial Least Squares Structural Equation Model (PLS-SEM) reveals the potential regulatory mechanism of the pioneer vegetation type on the soil multifunctionality in riparian sand mining sites. The numbers beside the arrows are the standardized path coefficients. Among them, the red lines represent positive effects, and the blue lines represent negative effects.

Discussion

This study revealed that in the extremely nutrient-poor substrates of riverbank sand mining sites, different pioneer vegetation types shaped distinct soil microbial communities through their functional traits. Furthermore, these trait patterns constituted the core environmental filters that screened microbial taxa, regulated

network structure, assembly processes, and functional potential, thereby supporting our first hypothesis.

This study uses a cross-sectional design with all plots have the same recovery duration (6 years). Following the space-for-time substitution approach (Miao et al., 2018; Lovell et al., 2023), we assume spatial differences among these vegetation types reflect potential successional trajectories, justified by identical mining history, and landscape position, minimizing confounding factors. Nonetheless, true successional dynamics require longitudinal sampling.

Pioneer Vegetation Types Shape Differentiated Soil Microbial Community Structure and Assembly Processes

Pioneer plants adapt to degraded environments through their life history strategies and functional traits, while profoundly influencing belowground ecological processes. Dong et al. (2023) found in alpine desert grasslands that different shrub types could influence soil microbial community succession either directly or indirectly through modification of soil substrates. The present study demonstrated that even in extremely degraded habitats such as riverbank sand mining sites characterized by strong abiotic filtering, different pioneer vegetation types were still capable of shaping distinct soil microbial communities. Notably, bacterial communities exhibited greater sensitivity to vegetation type than fungal communities (PERMANOVA, $p < 0.001$), consistent with findings by He et al. (2023) in arid and semi-arid ecosystems of Xinjiang Uygur Autonomous Region, China. Bacteria, with shorter life cycles, response more rapidly to root exudates and labile carbon (Feng et al. 2022; Lei et al. 2023), whereas fungi depend more on long-term organic matter accumulation and host specificity (Dickie et al. 2013; Frey. 2019).

Differences in dominant microbial taxa among vegetation types revealed the filtering effects of plant functional traits on microbial communities through modification of the rhizosphere microenvironment. The significant enrichment of *Actinobacteriota* in *A. scoparia* communities aligns with previous observations of high nitrogen and phosphorus contents in plant tissues of this species, as well as elevated ammonium nitrogen and total phosphorus levels in the soil. *Actinobacteriota* encompass numerous metabolically diverse taxa, many of which can rapidly utilize available nitrogen and phosphorus (Bhatti et al. 2017; AbdElgawad et al. 2020; Javed et al. 2021). As an annual pioneer species, *A. scoparia* may create relatively nutrient-rich micro-patches in the rhizosphere through input of high-nitrogen, high-phosphorus tissues, thereby selectively enriching these microbial taxa (Yang et al. 2024; Gong et al. 2025). Conversely, the significant enrichment of *Basidiomycota* in solitary tree plots, likely dominated by *ectomycorrhizal* fungi (consistent with fungal functional predictions) directly reflects the life strategy of woody plants adapting to nutrient-poor habitats through establishment of mycorrhizal symbioses to expand nutrient acquisition ranges. This also provides a biological explanation for the higher soil carbon-to-nitrogen ratios observed (Shi et al. 2023; Guo et al. 2024). The enrichment of *Nitrospirota* in *I. cylindrica* communities was directly associated with the high soil carbon-to-nitrogen ratio environment, suggesting that nitrification processes may represent a key component of nitrogen cycling under these conditions (Mosley et al. 2024; Wang et al. 2024). Notably, keystone taxa in *I. cylindrica* communities were predominantly *Acidobacteriota* subgroups, which have been found to be highly associated with nitrogen cycling processes in degraded ecosystems (Guo et al. 2022). These results support that even under strong abiotic filtering, the biological effects of pioneer vegetation can significantly direct microbial community compositional differentiation.

More importantly, functional prediction analysis revealed that these differences in community structure suggested potential heterogeneity in key ecosystem functions. Bacterial community function potentials were predominantly centered on nitrogen cycling processes, with different vegetation types regulating distinct nitrogen transformation pathways. The lower potentials for *aerobic ammonia oxidation* and

nitrification under *I. cylindrica* may be related to its more efficient nitrogen uptake capacity as a grass species, reducing ammonium substrate availability in the rhizosphere (Shinano et al. 1994; Yang et al. 2023; Yang et al. 2024). Conversely, the higher potentials for *nitrate/nitrite denitrification* under *I. cylindrica* and solitary tree plots suggest more frequent occurrence of anoxic microsites in these vegetation types (beneath tree litter or within dense grass root systems), promoting gaseous nitrogen losses (Myszograj.2018; McCoy et al. 2024). This differential regulation of nitrogen cycling pathways indicates that pioneer species may influence the balance of soil nitrogen availability, retention, and loss during early restoration stages.

Pioneer vegetation not only screens microorganisms through modification of resource environments but also regulates community assembly processes by shaping habitat physical structure and spatial heterogeneity, ultimately potentially contributing to the long-term development and stability of ecosystem functions under different restoration pathways (Richter-Heitmann et al. 2020; Barnett et al. 2020). Stochastic and deterministic processes represent two important and complementary mechanisms describing soil microbial community assembly, which can distinguish microbial preferences and adaptations to different habitats (Mori et al. 2018; Zhao et al. 2021). In this study, null model analysis further revealed that the dominant mechanisms of community assembly were closely associated with the microenvironments shaped by pioneer vegetation types. For bacterial communities, assembly in *A. scoparia* and *S. arundinaceum* was dominated by homogeneous selection (deterministic processes), potentially attributable to the relatively homogeneous soil chemical environments with strong selective pressure created by these species through root exudates or litter inputs, resulting in consistent filtering of bacterial taxa (Yan et al. 2018). Conversely, stochastic processes (dispersal limitation, variable selection) contributed more substantially in *I. cylindrica* and solitary tree plots, likely related to the relatively developed root systems of these vegetation types, which create more spatially heterogeneous habitat patches, allowing stochastic dispersal and local accidental events to play more important roles in community assembly (Pot et al. 2022). Compared with bacteria, fungal communities exhibited stochastic processes (dispersal limitation) as the dominant mechanism in most vegetation types. This may reflect, on one hand, the stronger host specificity and greater randomness of spore dispersal in fungal colonization (particularly mycorrhizal fungi) (Paz et al. 2021). On the other hand, it also indicates that during early successional stages, fungal communities have not yet established stable, obligate symbiotic relationships with plants. An exception was observed in *S. arundinaceum* communities, where fungal assembly processes were dominated by deterministic mechanisms. This would result from species-specific root exudate or unique rhizosphere conditions created by this perennial grass, which may exert strong selective pressure on fungal taxa (Mirshad and Puthur. 2016). However, given the moderate sample size (n = 8 per vegetation type) and cross-section design of this study, we cannot exclude the possibility that this pattern reflects stochastic variation or limited replication rather than a true signal. Further studies with large sample sizes and experimental manipulation are needed to confirm whether this deterministic assembly is a consistent feature of *S. arundinaceum* rhizosphere fungal.

Soil Physicochemical Properties Serve as Key Environmental Filters Driving Microbial Community Differentiation

The soil-vegetation interaction during ecological restoration in mining areas represents a highly complex process, constrained not only by local environmental factors but also influenced by soil and vegetation types (Chang et al. 2022; Barnett et al. 2020). The present study revealed that although pioneer vegetation types served as significant drivers of microbial community differentiation, their effects were largely mediated through modification and alteration of soil physicochemical properties. Redundancy

analysis (RDA) demonstrated that total carbon (TC), total phosphorus (TP), and nitrate nitrogen (NO_3-N) were the most important environmental factors explaining bacterial community variation, whereas fungal communities were closely associated with total carbon (TC), total phosphorus (TP), and protease (Prot) (Fig. 3A). These results directly support our second hypothesis and reveal that in the unique habitat of riverbank sand mining sites, the availability of carbon, nitrogen, and phosphorus constitutes the primary abiotic pressure filtering microbial taxa. We also acknowledge that unmeasured environmental factors (e.g., microtopography, soil texture, redox potential) may share variance with the identified drivers, potentially inflating their apparent unique contribution.

Previous studies have established that nitrogen limitation is a key factor driving community succession in degraded ecosystems (Zhang et al. 2015; Luo et al. 2025). In this study, the driving effects of soil nitrogen forms and transformation dynamics on bacterial communities were particularly pronounced. Bacterial community diversity exhibited significant negative correlations with TP and NO_3-N. Higher nitrate nitrogen levels are often associated with active nitrification, which may create a more eutrophic and competitive microenvironment, paradoxically inhibiting the diversity of certain bacterial taxa. This finding is consistent with some observations in nitrogen deposition studies (Xi et al. 2022; Li et al. 2023). For fungal communities, total carbon (TC) showed a significant positive correlation with diversity, emphasizing that organic carbon availability serves as a key limiting factor for fungal colonization and development during early succession. Carbon sources provided by litter inputs and root exudates supply the energetic basis for saprotrophic and symbiotic fungi (Rineau et al. 2013). The strong *ectomycorrhizal* function predicted signal detected in solitary tree plots may be closely related to their higher soil carbon-to-nitrogen ratios, as the establishment and maintenance of mycorrhizal symbioses require substantial photosynthetic carbon investment from host plants (Smith et al. 2009; Bell et al. 2024). We note that this carbon limitation may be specific to the early-successional, *saprotroph* dominate fungal communities in our system; in more advanced vegetation patches or mycorrhizal dominated systems, fungal communities can also be limited by nitrogen availability (Bashian-Victoroff et al. 2024)

In the extremely nutrient-poor substrates of sand mining sites, where initial organic matter is nearly absent and soil structure is homogeneous, the primary effect of pioneer vegetation colonization is to disrupt this abiotic homogeneity by creating nutrient “hotspots” through litter inputs and root activities. Consequently, microbial community assembly during early restoration represents a process strongly dominated by environmental filtering. Through their differentiated engineering effects, various vegetation types alter soil chemical properties (e.g., C:N:P stoichiometry) at different rates and through different pathways, thereby shaping distinct microbial habitats (He et al. 2023).

Microbial Interaction Network Structure and Stability Explain the Potential Resilience of Early Restoration Ecosystems

Microbial co-occurrence networks provide insights into community functional dynamics that extend beyond species composition (Codello et al. 2022; Peng et al. 2025). In this study, all networks were predominantly characterized by positive connections, indicating that in the stressful habitat of riverbank sand mining sites, microbial communities tend to establish potential cooperative or symbiotic relationships to collectively cope with resource limitations and environmental pressures. This finding is consistent with numerous studies in degraded ecosystems (Guo et al. 2022; Gao et al. 2023). Additionally, all networks exhibited high clustering coefficients and modular structures, displaying “small-world” network characteristics. Such network architecture is considered to enhance ecosystem functional redundancy and resistance to

environmental disturbances (Chen et al. 2020; Li and Zhang. 2025).

The cohesion metric provide insight into potential interaction regimes within microbial communities. Positive cohesion is thought to reflect cooperative interactions (e.g., resource sharing, metabolite exchange), whereas negative cohesion indicates competitive or inhibitory relationship (Herren and McMahon. 2017; Yuan et al. 2021). In our study, the high positive and low negative cohesion in *S. arundinaceum* bacterial communities, suggest a predominance of cooperative interactions, which may enhanced community stability and resistance to disturbance (Bu and Pandit. 2022). This may be attributed to *S. arundinaceum* as a perennial grass whose dense fibrous root system continuously inputs readily decomposable carbon sources, providing abundant public resources for cooperative microbial communities and thereby reducing competitive pressure among taxa for limited resources (Mirshad and Puthur. 2016). In contrast, the high negative cohesion observed in *A. scoparia* bacterial communities, combined with the highly modular characteristics of its fungal network, implies stronger competition pressure, possibly due to resource limitation or niche differentiation. This may relate to the life history strategy of *A. scoparia* as an annual pioneer species capable of directly colonizing soils following moss crust formation. The relatively high local nutrient availability may stimulate more intense microbial competition, prompting the formation of highly differentiated functional modules adapted to distinct niches, thereby maintaining overall functional stability (Yang et al. 2024; Gong et al. 2025). The fungal network under *I. cylindrica* exhibited the highest levels of both positive and negative cohesion, suggesting intense but balanced microbial interactions in the rhizosphere. This dynamic equilibrium may represent a strategy for adapting to nutrient-poor and disturbed environments (Jia et al. 2020).

Regulatory Pathways of the Plant-Soil-Microbe Continuum on Soil Multifunctionality

The restoration of degraded ecosystems is manifested in the reconstruction of soil multifunctionality (Chen et al. 2023). However, due to the asynchronous recovery processes between aboveground and belowground ecosystems, accurately assessing belowground restoration quality remains challenging (Liu et al. 2022; Song et al. 2024). Contrary to our initial hypothesis, microbial community composition and diversity exerted no direct effects on multifunctionality, while soil physical properties played a central mediating role. Specifically, vegetation type indirectly regulated soil multifunctionality through soil physical properties, but this pathway exhibited opposite directions in bacterial and fungal models. Vegetation type positively affected soil physical properties, with a negative subsequent effect on multifunctionality in the bacterial model, whereas in the fungal model, vegetation type negative affected soil physical properties, with a positive subsequent effect on multifunctionality. We caution that these opposite path signs should not be interpreted as temporal successional sequences due to the cross-sectional design.

This finding suggests that during early restoration stages in riverbank sand mining sites, a key ecological functional effect of pioneer vegetation is the rapid improvement of soil physical structure through pathways such as root penetration and litter coverage, rather than immediately driving microbe-mediated biogeochemical processes. This observation aligns with strategies for improving extremely nutrient-poor soil environments (Arocena et al. 2010; Gong et al. 2024). The absence of a direct microbial-multifunctionality link, while surprising given previous reports of close associations between microbial community characteristics and multifunctionality (Wang et al. 2024; Li et al.2025, Li et al. 2024), may reflect the early successional stage of our sites, where microbial communities have not yet developed sufficient function capacity to directly influence multifunctionality. Alternatively, the strong environmental filtering in sand mining sites could constrain microbial function expression, temporarily decoupling community

composition from ecosystem processes (Chen et al. 2022; Zhong et al. 2025). Longitudinal studies or manipulative experiments are needed to test whether a direct microbial effect emerges over longer recovery timescales.

This study provides important insights into the mechanisms underlying early restoration of riverbank sand mining sites; however, several limitations should be acknowledged. First, this study employed a cross-sectional space-for-time substitution approach with a single recovery duration (6 years); while all plots share identical mining history and landscape position, this design cannot confirm true successional dynamics, and inferred pathways should be viewed as correlative. Second, our sample size is moderate (n = 32) and the study was conducted at a single site along the Huai River, limiting generalizability to other regions or disturbance intensities. Third, functional predictions based on FAPROTAX and FUNGuild reflect taxonomic-based metabolic potential rather than directly measured process rates or gene expression. Fourth, plant functional traits (e.g., root architecture, litter C:N) were not directly measured. Future studies with longitudinal monitoring, experimental manipulation, and multi-site replication are needed to validate our findings.

Conclusions

In summary, this study demonstrates that in riverbank sand mining sites subjected to severe anthropogenic disturbance, naturally colonizing pioneer vegetation functions not only as a vanguard of surface landscape recovery but also as an important regulator of belowground ecosystem restoration. Through their differentiated life history strategies, these pioneer species modify the soil microenvironment and resource inputs, thereby filtering and shaping soil microbial communities that exhibit distinct structures, assembly processes, and stability characteristics. During the early stages of restoration, vegetation promotes soil multifunctionality primarily through physical improvement pathways. The differentiated microbial communities thus established provide the ecological foundation for subsequent functional divergence of ecosystem processes in later successional stages. Therefore, in riparian ecological restoration practices, the deliberate selection and configuration of pioneer vegetation with diverse functional traits may represent a potential strategy for promoting ecosystem recovery and enhancing ecosystem services based on microbial ecological principles.

Acknowledgements We thank Dr Zelong Yu for his assistance in plant species identification.

Contribution All authors contributed to the study conception and design. Material preparation, sediment collection and analysis were performed by all authors. The first draft of the manuscript was written by Xiang Lv and all authors commented on previous versions of the manuscript. All authors have read and approved the final manuscript.

Funding This work was supported by Xinyang Academy of Ecological Research Open Foundation (2023XYMS13), and the Natural Science Foundation of Henan Province (262300420128).

Declarations of interests The authors declare that they have no conflict of interest.

Ethics & declarations Plant species were formally identified by Zelong Yu (Xinyang Agriculture and Forest University) based on morphological characters following *Flora of Henan Province* (Henan Science and Technology Press, 2019). Voucher specimens of the three species have been deposited in the Xinyang Agriculture and Forest University under accession numbers XYAFU-2025-014.

All plant collections were carried out in compliance with relevant institutional, national, and

international guidelines and legislation. None of the collected species is listed as endangered under the IUCN Red List or CITES appendices. The study site is a degraded riparian sand mining area without restricted access. This study adheres to the IUCN Policy Statement on Research Involving Species at Risk of Extinction and the Convention on International Trade in Endangered Species of Wild Fauna and Flora (CITES).

Reference

AbdElgawad H, Abuelsoud W, Madany MM, Selim S, Zinta G, Mousa AS, Hozzein WN (2020) Actinomycetes enrich soil rhizosphere and improve seed quality as well as productivity of legumes by boosting nitrogen availability and metabolism. Biomolecules, 10(12): 1675. https://doi.org/10.3390/biom10121675

Akanwa AO (2020) River sand mining and its ecological footprint at Odor River, Nigeria. In: Agroecological footprints management for sustainable food system. Springer, Singapore, pp 473-514.

Arocena JM, Van Mourik JM, Schilder ML, Faz Cano A (2010) Initial soil development under pioneer plant species in metal mine waste deposits. Restoration Ecology, 18: 244-252. https://doi.org/10.1111/j.1526-100X.2009.00582.x

Azeria ET, Santala K, McIntosh AC, Aubin I (2020) Plant traits as indicators of recovery of reclaimed wellsites in forested areas: Slow but directional succession trajectory. Forest Ecology and Management, 468: 118180. https://doi.org/10.1016/j.foreco.2020.118180

Barnett SE, Youngblut ND, Buckley DH (2020) Soil characteristics and land-use drive bacterial community assembly patterns. FEMS Microbiology Ecology, 96(1): fiz194. https://doi.org/10.1093/femsec/fiz194

Bell CA, Magkourilou E, Ault JR, Urwin PE, Field KJ (2024) Phytophagy impacts the quality and quantity of plant carbon resources acquired by mutualistic arbuscular mycorrhizal fungi. Nature Communications 15(1): 801. https://doi.org/10.1038/s41467-024-44894-3

Bashian-Victoroff C, D.Yanai R, R.Horton T, J.Lanmit L (2024) Nitrogen and phosphorus additions affect fruiting of ectomycorrhizal fungi in a temperate hardwood forest. Fungal ecology 73:101388

Bhaduri D, Sihi D, Bhowmik A, Verma BC, Munda S, Dari B (2022) A review on effective soil health bio-indicators for ecosystem restoration and sustainability. Frontiers in Microbiology 13: 938481. https://doi.org/10.3389/fmicb.2022.938481

Bhatti AA, Haq S, Bhat RA (2017) Actinomycetes benefaction role in soil and plant health. Microbial Pathogenesis 111:458-467. https://doi.org/10.1016/j.micpath.2017.09.036

Bu Y, Pandit A (2022) Cohesion mechanisms for bioadhesives. Bioactive Materials 13: 105-118. https://doi.org/10.1016/j.bioactmat.2021.11.008

Byrnes JE, Gamfeldt L, Isbell F, Lefcheck JS, Griffin JN, Hector A, Cardinale BJ, Hooper DU, Dee LE, Emmett Duffy J (2014) Investigating the relationship between biodiversity and

ecosystem multifunctionality: challenges and solutions. Methods in Ecology and Evolution 5(2): 111-124. https://doi.org/10.1111/2041-210X.12143

Cabrera Rodríguez F, Otto R, Fernández-Palacios JM (2022) Changes in soil chemical properties and plant species composition during primary succession on an oceanic island. Journal of Vegetation Science 33(3): e13137. https://doi.org/10.1111/jvs.13137

Cacace C, García-Gil JC, Cocozza C, De Mastro F, Brunetti G, Traversa A (2022) Effects of different pioneer and exotic species on the changes of degraded soils. Scientific Reports 12(1): 18548. https://doi.org/10.1038/s41598-022-21753-9

Chang Y, Chen F, Zhu Y, You Y, Cheng Y, Ma J (2022) Influence of revegetation on soil microbial community and its assembly process in the open-pit mining area of the Loess Plateau, China. Frontiers in Microbiology 13: 992816. https://doi.org/10.3389/fmicb.2022.992816

Chen J, Nan J, Xu D, Mo L, Zheng Y, Chao L, Qu H, Guo Y, Li F, Bao Y (2020) Response differences between soil fungal and bacterial communities under opencast coal mining disturbance conditions. Catena 194: 104779. https://doi.org/10.1016/j.catena.2020.104779

Chen J, Wang P, Wang C, Wang X, Miao L, Liu S, Yuan Q, Sun S (2020) Fungal community demonstrates stronger dispersal limitation and less network connectivity than bacterial community in sediments along a large river. Environmental Microbiology 22(3): 832-849. https://doi.org/10.1111/1462-2920.14752

Chen Y, Chi J, Lu X, Cai Y, Jiang H, Zhang Q, Zhang K (2023) Fungal-bacterial composition and network complexity determine soil multifunctionality during ecological restoration. Catena 230: 107251. https://doi.org/10.1016/j.catena.2023.107251

Chen Y, Li W, You Y, Ye C, Shu X, Zhang Q, Zhang K (2022) Soil properties and substrate quality determine the priming of soil organic carbon during vegetation succession. Plant and Soil 471(1): 559-575. https://doi.org/10.1007/s11104-021-05240-0

Ciccazzo S, Esposito A, Rolli E, Zerbe S, Daffonchio D, Brusetti L (2014) Different pioneer plant species select specific rhizosphere bacterial communities in a high mountain environment. SpringerPlus 3(1): 391. https://doi.org/10.1186/2193-1801-3-391

Codello A, Hose GC, Chariton A (2022) Microbial co-occurrence networks as a biomonitoring tool for aquatic environments: a review. Marine and Freshwater Research 74(5): 409-422. https://doi.org/10.1071/MF22039

Dickie IA, Martínez-García LB, Koele N, Grelet GA, Tylianakis JM, Peltzer DA, Richardson SJ (2013) Mycorrhizas and mycorrhizal fungal communities throughout ecosystem development. Plant and Soil 367(1): 11-39. https://doi.org/10.1007/s11104-013-1609-0

Deng Y, Jiang Y H, Yang Y, He Z, Luo F, Zhou, J. (2012) Molecular ecological network analyses. BMC bioinformatics 13(1): 113. https://doi.org/10.1186/1471-2105-13-113

Dong R, Wang X, Wang Y, Ma Y, Yang S, Zhang L, Qin J, Quzha R (2023) Differences in soil microbial communities with successional stage depend on vegetation coverage and soil substrates in alpine desert shrublands. Plant and Soil 485(1): 549-568. https://doi.org/10.1007/s11104-022-05812-8

Esperschütz J, Zimmermann C, Dümig A, Welzl G, Buegger F, Elmer M, Munch JC, Schloter M (2013) Dynamics of microbial communities during decomposition of litter from pioneering plants in initial soil ecosystems. Biogeosciences 10(7): 5115-5124. https://doi.org/10.5194/bg-10-5115-2013

Feng J, He K, Zhang Q, Han M, Zhu B (2022) Changes in plant inputs alter soil carbon and microbial communities in forest ecosystems. Global Change Biology 28(10): 3426-3440. https://doi.org/10.1111/gcb.16107

Frey SD (2019) Mycorrhizal fungi as mediators of soil organic matter dynamics. Annual Review of Ecology, Evolution, and Systematics 50(1): 237-259. https://doi.org/10.1146/annurev-ecolsys-110617-062331

Fritts R (2019) The world needs to get serious about managing sand, U.N. report says. Science. https://doi.org/10.1126/science.aay1281

Gao L, Wang W, Liao X, Tan X, Yue J, Zhang W, Wu J, Willison JH, Tian Q, Liu Y (2023) Soil nutrients, enzyme activities, and bacterial communities in varied plant communities in karst rocky desertification regions in Wushan County, Southwest China. Frontiers in Microbiology 14: 1180562. https://doi.org/10.3389/fmicb.2023.1180562

Ge Z, Zhang X, Liu C, Li M, Wang R, Zhang Y, Zhang, Z. (2025) Microbial determinants of soil quality in mixed larch and birch forests: network structure and keystone taxa abundances. *Fron*tiers in Plant Science, 16: 1491038. https://doi.org/10.3389/fpls.2025.1491038

Gong C, Ni D, Liu Y, Li Y, Huang Q, Tian Y, Zhang H (2024) Herbaceous vegetation in slope stabilization: A comparative review of mechanisms, advantages, and practical applications. Sustainability 16(17): 7620. https://doi.org/10.3390/su16177620

Gong H, Duan D, Suo Y, Jia N, Hu K, Chen J, Hu N, Zhao G, Wang Z (2025) Conservative allocation strategy of nitrogen and phosphorus among leaves, stems and roots of Artemisia species. BMC Plant Biology 25(1): 182. https://doi.org/10.1186/s12870-024-06019-8

Graziano MP, Deguire AK, Surasinghe TD (2022) Riparian buffers as a critical landscape feature: insights for riverscape conservation and policy renovations. Diversity 14(3): 172. https://doi.org/10.3390/d14030172

Guo L, Deng M, Li X, Schmid B, Huang J, Wu Y, Peng Z, Yang L, Liu L (2024) Evolutionary and ecological forces shape nutrient strategies of mycorrhizal woody plants. Ecology Letters 27(1): e14330. https://doi.org/10.1111/ele.14330

Guo Y, Wu J, Yu Y (2022) Differential response of soil microbial community structure in coal mining areas during different ecological restoration processes. Processes 10(10): 2013. https://doi.org/10.3390/pr10102013

He J, Qi R, Wang S, Duan X, Meng L, Ai S, Yu L, Gadd GM, Song W (2023) Distinct composition patterns of bacterial and fungal communities and biogeochemical cycling genes depend on the vegetation type in arid soil. Applied Soil Ecology 191: 105064. https://doi.org/10.1016/j.apsoil.2023.105064

Herren CM, McMahon KD (2017) Cohesion: a method for quantifying the connectivity of microbial communities. The ISME Journal 11(11): 2426-2438. https://doi.org/10.1038/ismej.2017.91

Hu A, Wang H, Cao M, Rashid A, Li M, Yu CP (2019) Environmental filtering drives the assembly of habitat generalists and specialists in the coastal sand microbial communities of Southern China. Microorganisms 7(12): 598. https://doi.org/10.3390/microorganisms7120598

Javed Z, Tripathi GD, Mishra M, Dashora K (2021) Actinomycetes–the microbial machinery for the organic-cycling, plant growth, and sustainable soil health. Biocatalysis and Agricultural Biotechnology 31: 101893. https://doi.org/10.1016/j.bcab.2020.101893

Jia T, Guo T, Chai B (2020) Bacterial community characteristics and enzyme activities in Imperata cylindrica litter as phytoremediation progresses in a copper tailings dam. PeerJ 8: e9612. https://doi.org/10.7717/peerj.9612

Koehnken L, Rintoul MS, Goichot M, Tickner D, Loftus AC, Acreman MC (2020) Impacts of riverine sand mining on freshwater ecosystems: A review of the scientific evidence and guidance for future research. River Research and Applications 36(3): 362-370. https://doi.org/10.1002/rra.3586

Lai J, Zou Y, Zhang J, Peres-Neto PR (2022) Generalizing hierarchical and variation partitioning in multiple regression and canonical analyses using the rdacca.hp R package. Methods in Ecology and Evolution 13(4): 782-788. https://doi.org/10.1111/2041-210X.13800

Lei X, Shen Y, Zhao J, Huang J, Wang H, Yu Y, Xiao C (2023) Root exudates mediate the processes of soil organic carbon input and efflux. Plants 12(3):630. https://doi.org/10.3390/plants12030630

Li J, Chen H, Guo K, Li W, Feng X, Liu X (2021) Changes in soil properties induced by pioneer vegetation patches in coastal ecosystem. Catena 204: 105393. https://doi.org/10.1016/j.catena.2021.105393

Li J, Wang X, Yuan M, Duan W, Xia J, Zhang X, Zhao Y, Wang J (2025) Effect of soil microbial community on ecosystem multifunctionality in an alpine grassland. Catena 249: 108714. https://doi.org/10.1016/j.catena.2024.108714

Li W, He E, Van Gestel CA, Peijnenburg WJ, Chen G, Liu X, Zhu D, Qiu H (2024) Pioneer plants enhance soil multifunctionality by reshaping underground multitrophic community during natural succession of an abandoned rare earth mine tailing. Journal of Hazardous Materials 472: 134450. https://doi.org/10.1016/j.jhazmat.2024.134450

Li Y, Zou N, Liang X, Zhou X, Guo S, Wang Y, Qin X, Tian Y, Lin J (2023) Effects of nitrogen input on soil bacterial community structure and soil nitrogen cycling in the rhizosphere soil of Lycium barbarum L. Frontiers in Microbiology 13: 1070817. https://doi.org/10.3389/fmicb.2022.1070817

Li Z, Zhang C (2025) Spatial evolution and resilience analysis of marine eco-environmental protection enterprises. Marine Pollution Bulletin 216: 117953. https://doi.org/10.1016/j.marpolbul.2025.117953

Liu M, He W, Zhang Z, Sun J, Cong N, Nie X, Wang Y, Zhang L, Yang B, Chen Y, Zhou H, Shao Y, Wang Y (2022) Mutual feedback between above-and below-ground controls the restoration of alpine ecosystem multifunctionality in long-term grazing exclusion. Journal of Cleaner Production 333: 130184. https://doi.org/10.1016/j.jclepro.2021.130184

Luo Y, Cheng J, Mahmood M, Wei S, Peng L, Zhang C, Zhang M, Zhang J, Yang H, Wang J, Hao Z, Yan X (2025) Plant community restoration time is a key factor affecting plant nutrient and species richness. Scientific Reports 15(1): 15752. https://doi.org/10.1038/s41598-025-97853-7

Lovell R S, Collins S, Martin S H, Pigot A L, Phillimore A B. (2023) Space-for-time substitutions in climate change ecology and evolution. Biological Reviews 98(6): 2243-2270.

Macieira BPB, Locosselli GM, Buckeridge MS, Hartmann H, Cuzzuol GRF (2020) Stem and leaf functional traits allow successional classification in six pioneer and non-pioneer tree species in Tropical Moist Broadleaved Forests. Ecological Indicators 113: 106254. https://doi.org/10.1016/j.ecolind.2020.106254

Markowicz A, Woźniak G, Borymski S, Piotrowska-Seget Z, Chmura D (2015) Links in the functional diversity between soil microorganisms and plant communities during natural succession in coal mine spoil heaps. Ecological Research 30(6): 1005-1014. https://doi.org/10.1007/s11284-015-1301-3

Martínez-Garza C, Campo J, Ricker M, Tobón W (2016) Effect of initial soil properties on six-year growth of 15 tree species in tropical restoration plantings. Ecology and Evolution 6(24): 8686-8694. https://doi.org/10.1002/ece3.2498

McCoy J, Chaffee M, Mittelstet A, Messer T, Comfort S (2024) Nitrate removal by floating treatment wetlands under aerated and unaerated conditions: Field and laboratory results. Nitrogen 5(4): 808-827. https://doi.org/10.3390/nitrogen5040054

Miao R, Qiu X, Guo M, Musa A, Jiang D. (2018) Accuracy of space-for-time substitution for

vegetation state prediction following shrub restoration. Journal of Plant Ecology 11(2): 208-217.

Miller HR, Lane SN (2019) Biogeomorphic feedbacks and the ecosystem engineering of recently deglaciated terrain. Progress in Physical Geography 43(1): 24-45. https://doi.org/10.1177/0309133318816536

Mirshad PP, Puthur JT (2016) Arbuscular mycorrhizal association enhances drought tolerance potential of promising bioenergy grass (Saccharum arundinaceum retz.). Environmental Monitoring and Assessment 188(7): 425. https://doi.org/10.1007/s10661-016-5428-7

Mori AS, Isbell F, Seidl R (2018) β-diversity, community assembly, and ecosystem functioning. Trends in Ecology & Evolution 33(7):549-564. https://doi.org/10.1016/j.tree.2018.04.012

Mosley OE, Gios E, Handley KM (2024) Implications for nitrogen and sulphur cycles: phylogeny and niche-range of Nitrospirota in terrestrial aquifers. ISME Communications 4(1): ycae047. https://doi.org/10.1093/ismeco/ycae047

Myszograj S (2018) Mechanisms of biological processes in domestic wastewater treatment plants. Civil and Environmental Engineering Reports 177-192. https://doi.org/10.2478/ceer-2018-0015

Ning, D., Yuan, M., Wu, L., Zhang, Y., Guo, X., Zhou, X., Yang, Y., Arkin, A., Firestone, M., Zhou, J. (2020). A quantitative framework reveals ecological drivers of grassland microbial community assembly in response to warming. Nature communications, 11(1), 4717.

Pandey S, Kumar G, Kumari N, Pandey R (2023) Assessment of causes and impacts of sand mining on river ecosystem. In: Hydrogeochemistry of aquatic ecosystems, pp 357-379.

Paz C, Öpik M, Bulascoschi L, Bueno CG, Galetti M (2021) Dispersal of arbuscular mycorrhizal fungi: evidence and insights for ecological studies. Microbial Ecology 81(2): 283-292. https://doi.org/10.1007/s00248-020-01596-x

Peddle SD, Hodgson RJ, Borrett RJ, Brachmann S, Davies TC, Erickson TE, Liddicoat C, Muñoz-Rojas M, Robinson JM, Watson CD, Krauss SL, Breed MF (2025) Practical applications of soil microbiota to improve ecosystem restoration: current knowledge and future directions. Biological Reviews 100(1): 1-18. https://doi.org/10.1111/brv.13124

Peng F, Wu B, Zheng Q, Long Y, Jiang J, Hu X (2025) Long-abandoned mining environments reshape soil microbial co-occurrence patterns, community assembly, and biogeochemistry. Applied Soil Ecology 213: 106254. https://doi.org/10.1016/j.apsoil.2025.106254

Pot V, Portell X, Otten W, Garnier P, Monga O, Baveye PC (2022) Understanding the joint impacts of soil architecture and microbial dynamics on soil functions: Insights derived from microscale models. European Journal of Soil Science 73(3): e13256.

https://doi.org/10.1111/ejss.13256

Qiu X, Cao G, Han G, Zhao Q, Cao S, Ji S (2025) Impact of vegetation type on taxonomic and functional composition of soil microbial communities in the Northeastern Qinghai–Tibet Plateau. Microorganisms 13(9): 2075. https://doi.org/10.3390/microorganisms13092075

Qiu Z, Li J, Wang P, Wang D, Han L, Gao X, Shu J (2023) Response of soil bacteria on habitat-specialization and abundance gradient to different afforestation types. Scientific Reports 13(1): 18181. https://doi.org/10.1038/s41598-023-45025-0

Qin Y, Yan T, Feng S. (2026) Influence of vegetation types on soil physicochemical and biochemical properties in naturally recovering riverbank sand mining sites. Scientific Reports 16: 12494 https://doi.org/10.1038/s41598-026-42081-2

Rentier ES, Cammeraat LH (2022) The environmental impacts of river sand mining. Science of the Total Environment 838: 155877. https://doi.org/10.1016/j.scitotenv.2022.155877

Richter-Heitmann T, Hofner B, Krah FS, Sikorski J, Wüst PK, Bunk B, Huang S, Regan KM, Berner D, Boeddinghaus RS, Marhan S, Prati D, Kandeler E, Overmann J, Friedrich MW (2020) Stochastic dispersal rather than deterministic selection explains the spatio-temporal distribution of soil bacteria in a temperate grassland. Frontiers in Microbiology 11: 1391. https://doi.org/10.3389/fmicb.2020.01391

Rineau F, Shah F, Smits MM, Persson P, Johansson T, Carleer R, Troein C, Tunlid A (2013) Carbon availability triggers the decomposition of plant litter and assimilation of nitrogen by an ectomycorrhizal fungus. The ISME Journal 7(10): 2010-2022. https://doi.org/10.1038/ismej.2013.91

Rousk J, Frey SD (2015) Revisiting the hypothesis that fungal-to-bacterial dominance characterizes turnover of soil organic matter and nutrients. Ecological Monographs 85(3): 457-472. https://doi.org/10.1890/14-1796.1

Shi J, Wang X, Wang E (2023) Mycorrhizal symbiosis in plant growth and stress adaptation: from genes to ecosystems. Annual Review of Plant Biology 74(1): 569-607. https://doi.org/10.1146/annurev-arplant-061722-090342

Shinano T, Osaki M, Yamada S, Tadano T (1994) Comparison of root growth and nitrogen absorbing ability between Gramineae and Leguminosae during the vegetative stage. Soil Science and Plant Nutrition 40(3): 485-495. https://doi.org/10.1080/00380768.1994.10413327

Singh R, Tiwari AK, Singh GS (2021) Managing riparian zones for river health improvement: an integrated approach. Landscape and Ecological Engineering 17(2): 195-223. https://doi.org/10.1007/s11355-020-00436-5

Smith FA, Grace EJ, Smith SE (2009) More than a carbon economy: nutrient trade and ecological sustainability in facultative arbuscular mycorrhizal symbioses. New Phytologist 182(2): 347-358. https://doi.org/10.1111/j.1469-8137.2008.02753.x

Song D, Hu Z, Zeng J, Sun H (2024) Influence of mining on vegetation in semi-arid areas of western China based on the coupling of above ground and below ground – A case study of Daliuta coalfield. Ecological Indicators 161: 111964. https://doi.org/10.1016/j.ecolind.2024.111964

Sun X, Zhou Y, Tan Y, Wu Z, Lu P, Zhang G, Yu F (2018) Restoration with pioneer plants changes soil properties and remodels the diversity and structure of bacterial communities in rhizosphere and bulk soil of copper mine tailings in Jiangxi Province, China. Environmental Science and Pollution Research 25(22): 22106-22119. https://doi.org/10.1007/s11356-018-2244-3

Torres A, Brandt J, Lear K, Liu J (2017) A looming tragedy of the sand commons. Science 357(6355): 970-971. https://doi.org/10.1126/science.aao0503

Venson GR, Marenzi RC, Almeida TCM, Deschamps-Schmidt A, Testolin RC, Rörig LR, Radetski CM (2017) Restoration of areas degraded by alluvial sand mining: use of soil microbiological activity and plant biomass growth to assess evolution of restored riparian vegetation. Environmental Monitoring and Assessment 189(3): 120. https://doi.org/10.1007/s10661-017-5852-3

Wang H, Chen K, Jin H, Hu R (2024) Interspecific differences in carbon and nitrogen metabolism and leaf epiphytic bacteria among three submerged macrophytes in response to elevated ammonia nitrogen concentrations. Plants 13(11): 1427. https://doi.org/10.3390/plants13111427

Wang J, Pan Z, Yu J, Zhang Z, Li YZ (2023) Global assembly of microbial communities. mSystems 8(3): e01289-22. https://doi.org/10.1128/msystems.01289-22

Wang X, Hou Y, Li H, Li Z, Zhang J, Bao T, Chao L, Minggagud H, Wang L, Liang C, Li FY (2024) Network complexity and community composition of key bacterial functional groups promote ecosystem multifunctionality in three temperate steppes of Inner Mongolia. Plant and Soil 494(1): 251-268. https://doi.org/10.1007/s11104-023-06266-2

Wu S, Liu Y, Southam G, Robertson LM, Wykes J, Yi Q, Hall M, Li Z, Sun Q, Saha N, Chan T, Lu Y, Huang L (2021) Rhizosphere drives biotite-like mineral weathering and secondary Fe–Si mineral formation in Fe ore tailings. ACS Earth and Space Chemistry 5(3): 618-631. https://doi.org/10.1021/acsearthspacechem.0c00320

Xi D, Jin S, Wu J (2022) Soil bacterial community is more sensitive than fungal community to canopy nitrogen deposition and understory removal in a Chinese fir plantation. Frontiers in Microbiology 13: 1015936. https://doi.org/10.3389/fmicb.2022.1015936

Yan J, Wang L, Hu Y, Tsang YF, Zhang Y, Wu J, Fu X, Sun Y (2018) Plant litter composition selects different soil microbial structures and in turn drives different litter decomposition pattern and soil carbon sequestration capability. Geoderma 319: 194-203. https://doi.org/10.1016/j.geoderma.2018.01.011

Yang H, Yu X, Song J, Wu J (2024) Artemisia smithii patches form fertile islands and lead to heterogeneity of soil bacteria and fungi within and around the patches in alpine meadows of the Qinghai-Tibetan Plateau. Frontiers in Plant Science 15: 1411839. https://doi.org/10.3389/fpls.2024.1411839

Yang J, Luo H, Wang H, Qin T, Yang M, Chen L, Wu X, He BJ (2024) Removal effect of pollutants from stormwater runoff in shallow bioretention system with gramineous plants. Water Science and Technology 89(8): 1946-1960. https://doi.org/10.2166/wst.2024.105

Yang P, Li X, Li C, Zhang J (2023) Effects of long-term exclosure on main plant functional groups and their biochemical properties in a patchily degraded alpine meadow in the source zone of the Yellow River, west China. Agronomy 13(11): 2781. https://doi.org/10.3390/agronomy13112781

Ying D, Chen X, Hou J, Zhao F, Li P (2023) Soil properties and microbial functional attributes drive the response of soil multifunctionality to long-term fertilization management. Applied Soil Ecology 192: 105095. https://doi.org/10.1016/j.apsoil.2023.105095

Yu T, Yang R, Jie X, Lian T, Zang H, Zeng Z, Yang Y (2024) Organic management improved the multifunctionality in recolonization soil by increasing microbial diversity and function. Functional Ecology 38(10): 2207-2219. https://doi.org/10.1111/1365-2435.14628

Yuan MM, Guo X, Wu L, Zhang YA, Xiao N, Ning D, Shi Z, Zhou X, Wu L, Yang Y, Tiedje J, Zhou J (2021) Climate warming enhances microbial network complexity and stability. Nature Climate Change 11(4): 343-348. https://doi.org/10.1038/s41558-021-00989-9

Zhalnina K, Louie KB, Hao Z, Mansoori N, Da Rocha UN, Shi S, Cho H, Karaoz U, Loqué D, Bowen BP, Firestone MK, Northen TR, Brodie EL (2018) Dynamic root exudate chemistry and microbial substrate preferences drive patterns in rhizosphere microbial community assembly. Nature Microbiology 3(4): 470-480. https://doi.org/10.1038/s41564-018-0129-3

Zhang M, O'Connor PJ, Zhang J, Ye X (2021) Linking soil nutrient cycling and microbial community with vegetation cover in riparian zone. Geoderma 384: 114801. https://doi.org/10.1016/j.geoderma.2020.114801

Zhang W, Zhao J, Pan F, Li D, Chen H, Wang K (2015) Changes in nitrogen and phosphorus limitation during secondary succession in a karst region in southwest China. Plant and Soil 391(1): 77-91. https://doi.org/10.1007/s11104-015-2406-8

Zhao Y, Liao J, Zhang Q, Chen J, Gong X, Shi Y, Shi M, Yang D, Fan S, Zhou X, Cao L, Hu, K. (2024). Development of China ground climate normal value dataset from 1991 to 2020. Chinese Journal of Atmospheric Sciences, 48(2): 555-571. https://doi.org/10.3878/j.issn.1006-9895.2204.22010

Zhao J, Ma J, Yang Y, Yu H, Zhang S, Chen F (2021) Response of soil microbial community to vegetation reconstruction modes in mining areas of the Loess Plateau, China. Frontiers

in Microbiology 12: 714967. https://doi.org/10.3389/fmicb.2021.714967

Zhong Y, Zhang B, Zhu Y, Shangguan Z, Li T, Deng L, Chen L, Yan W (2025) Shifts in the fungal community promote soil carbon accumulation in microaggregates during long-term secondary succession. Functional Ecology 39(8): 2029-2043. https://doi.org/10.1111/1365-2435.70018

Zhu SC, Zheng HX, Liu WS, Liu C, Guo MN, Huot H, Morel JL, Qiu R, Chao Y, Tang YT (2022) Plant-soil feedbacks for the restoration of degraded mine lands: A review. Frontiers in Microbiology 12:751794. https://doi.org/10.3389/fmicb.2021.751794